

We thank the referees for their reviews and Dr. Andrew Lambe and coworkers for their contributed short comment. To facilitate the review process we have copied the reviewer comments in black text. Our responses are in regular blue font. We have responded to all the referee comments and made alterations to our paper (**in bold text**). Figures, tables, equations, and sections in the responses are numbered as in the *revised* manuscript unless specified, while page and line numbers refer to the AMTD paper.

Anonymous Referee #1

The manuscript entitled, “HOx radical chemistry in oxidation flow reactors with low pressure mercury lamps systematically examined by modeling,” by Peng et al. describes an extensive set of kinetics calculations on the oxidative environment of the Potential Aerosol Mass (PAM) flow reactor. A standard chemical kinetic plug flow model is used to characterize the chemical environment of the PAM reactor, which could ultimately lead to a more robust interpretation and design of both field and laboratory based experiments. The model is clearly presented and differences between 185 nm and 254 nm photolysis is compared and evaluated in nice detail. I applaud the authors for undertaking what is clearly a comprehensive and very time consuming study, which hopefully will be valued by the community of users (which is quite extensive) of the PAM reactor.

R1.1) One of the main “outputs” of this detailed mechanistic study appears to be simple analytical expressions (eq. 5 and 6) that allows one to compute the OH exposure directly from H₂O, UV, O₃, etc. In particular eq. 6 relates the exposure to measurements of ozone before and after the reactor. This equation seems to distill much of the detailed work presented in the paper and also may be of most interest to current research groups that use the PAM. The authors should better clarify for the community the assumptions of using this equation in practice. For example, this parametrization (derived from the modeling) assumes plug flow conditions at which in reality the PAM reactor is clearly not. What errors are incurred if this equation is directly used for the real device?

We have added the following text to the paper to address the limitations of the OH estimation equation:

“We expect that the functional form of these equations will apply to OFR254 setups operated from other researchers, given the common drivers and chemistry. However the numerical values of the coefficients may vary for, e.g., reactors of different geometries. We recommend always refitting the estimation equations to data for the system of interest (e.g., using experimental VOC decay curves), and reporting them in the literature (e.g., Palm et al., 2015). We also note that the residence time is assumed as 180 s for our equations. As a first-order estimate, the OH_{exp} should be multiplied by RT/180, where RT is the residence time used in s. This RT correction will have an error smaller than the uncertainties in the model except under extreme cases of very short residence times or large OH suppression.”

To improve the section on the OH estimation equation, we have modified text at P3909/L5 to:

“An equation was reported for OFR185 in which OH_{exp} is estimated from H_2O and OHR_{ext} inputs and O_3 output ($\text{O}_{3,\text{out}}$), with the latter parameter serving as a surrogate of UV intensity (Li et al., 2015). The full equation is shown as below

$$\log \text{OH}_{\text{exp}} = 26.89 + (-1.7629 - 1.2947 \cdot \text{OHR}_{\text{ext}}^{0.076549} + 0.14469 \cdot \log \text{O}_{3,\text{out}} \cdot \text{OHR}_{\text{ext}}^{0.046}) \cdot \log \text{O}_{3,\text{out}} + \log \text{H}_2\text{O}. \quad (10)$$

We have also modified text at P3911/L2 to:

“The OH_{exp} estimation equation proposed by Li et al. (2015) for OFR185 avoided an explicit dependence on UV by using instead O_3 as its surrogate, since in OFR185 this species is only *formed* by the 185nm radiation. We follow a similar approach to derive an alternative estimation equation for OH_{exp} in OFR254 in which the logarithm of the ratio of the output to input O_3 ($\log r\text{O}_3 = \log (\text{O}_{3,\text{out}}/\text{O}_{3,\text{in}})$) is used as a surrogate of UV, as well as H_2O , since both photons and HO_x produced from H_2O *destroy* O_3 . OH_{exp} can then be expressed as a function of only $r\text{O}_3$, OHR_{ext} , and $\text{O}_{3,\text{in}}$:

$$\log \text{OH}_{\text{exp}} = a - \log(-\log r\text{O}_3) + b(\text{OHR}_{\text{ext}}/\text{O}_{3,\text{in}})^c \quad (12)$$

where a – c are fitting parameters. Their values are reported in Table S2. Obviously, Eq. 12, with only 3 input variables and 3 parameters, is much simpler than Eq. 11.

Furthermore, the mean absolute value of the relative deviation between OH_{exp} estimated by Eq. 12 and computed by the full model is only 9%, and the scatter in the relationship is substantially smaller than for Eq. 11 (Fig. 12b). O_3 can be easily monitored in OFR254 experiments at both the entrance and the exit of the OFR with a single O_3 analyzer and a switching valve system. Therefore, we recommend measuring both O_3 input and output concentrations in OFR254 experiments to more simply and accurately estimate OH_{exp} . Note that a good experimental determination of $r\text{O}_3$ requires that a measurable amount of O_3 is destroyed, but also that some O_3 still remains at the reactor output. We estimate this range as corresponding to $r\text{O}_3$ between 0.05 and 0.95. However, $r\text{O}_3 > 0.95$ (i.e., only <5% of $\text{O}_{3,\text{in}}$ is destroyed in the OFR) only occurs under low H_2O and/or UV conditions, where OH_{exp} is also very low and may be of limited experimental interest, while $r\text{O}_3 < 0.05$ occurs rarely, i.e., only at the highest H_2O and UV that we explored. For experiments where $r\text{O}_3$ is very low or close to 1, Eq. 11 can be applied to estimate OH_{exp} .

The good performance of Eq. 12 can be explained by a key relationship between OH_{exp} and $r\text{O}_3$. Note that the last term in Eq. 12 is minor: $b(\text{OHR}_{\text{ext}}/\text{O}_{3,\text{in}})^c$ generally ranges 0.5–1, while $-\log r\text{O}_3$ spans orders of magnitude. Thus, $\log \text{OH}_{\text{exp}}$ is approximately proportional to $\log (-\log r\text{O}_3)$, which already captures effects of both H_2O and UV, as well as partial effects of OHR_{ext} and $\text{O}_{3,\text{in}}$. The last term in Eq. 12 can be regarded as a minor correction. Using the destruction of O_3 is conceptually similar to estimating OH_{exp} by measuring the decay of conventional OH reactants, e.g., SO_2 and CO . To estimate OH_{exp} , we utilize the relationship that the loss of reactant molecules is proportional to OH_{exp} and their rate constant. However, when O_3 destruction is used as the basis for OH_{exp}

estimation, the relationship is somewhat different. An approximate proportional relationship still holds between gross consumed OH and net consumed O₃, hence also between OH_{exp} and log rO₃.”

For the discussion of non-plug flow, see response to comment R1.2 below.

R1.2) Related to point 1. What differences would be expected for OFR's that are not plug flow (e.g. PAM). A paragraph should be included to address this point so it is clear to the reader that the kinetic modeling, error analysis and estimation presented in the manuscript are for an “idealized” system and not a direct simulation of PAM.

This issue had already been partially addressed by Li et al. (2015) with the following text (their p. 4421): “A distribution of residence times in the reactor has been published,¹⁸ and the average OH exposure calculated from the model using the residence time distribution (RTD) is not significantly different from that with the plug-flow approximation (Figure S2, Supporting Information). For the typical conditions, the average OH exposure calculated with RTD is 10% higher than that with plug flow, which is smaller than the model uncertainty (a factor of 2).”

We hoped to limit the scope of the present manuscript that is already long and complex, and perform a more detailed exploration of the effect of the residence time distribution in a future publication, since we expected that it would require significant space and detail to do so. However since both reviewers asked for more detail about this issue, we have performed a systematic exploration of this topic and added a new section and several figures, which are copied below. We note that indeed the added text and figures would have represented a significant fraction of a separate publication, consistent with our initial assessment.

“3.5 Effect of non-plug flow

In most of this paper we use the plug flow assumption to allow interpreting any trends as being due to chemistry only. However, it is of interest to evaluate the impact of a non-plug flow RTD over a wider range of conditions. Li et al. (2015) reported, for a typical OFR185 case, a 10% change in average OH_{exp} when using the residence time distribution (RTD) reported by Lambe et al. (2011a). An OFR with a complex RTD can be approximately simulated as a set of plug-flow OFRs with different residence times. We thus calculate the outputs (i.e., OH_{exp}, O₃, SO₂ etc.) as a function of residence time using our plug-flow model, then compute their average values as the weighted average according to a specified RTD. A more complete simulation would involve the use of Computational Fluid Dynamics software, along with diffusion and the three-dimensional UV light fields, which is outside the scope of the present paper.

We perform the calculations for OFR185, OFR254-70, and OFR254-7. In each case we simulate two RTDs, one for fully developed laminar flow in a cylindrical tube (Mory, 2013), and the measured PAM RTD reported in Lambe et al. (2011a), shown in Figure S8. The use of both non-plug flow RTDs allows a first evaluation of the importance of the shape of the RTD on the results. This is useful since some OFRs such as TPOT (George

et al., 2007) are closer to a cylindrical tube, and also since some field applications of the PAM OFR do not use an inlet plate (Ortega et al., 2013, 2015) and are expected to have a less skewed RTD than reported by Lambe et al. (2011a).

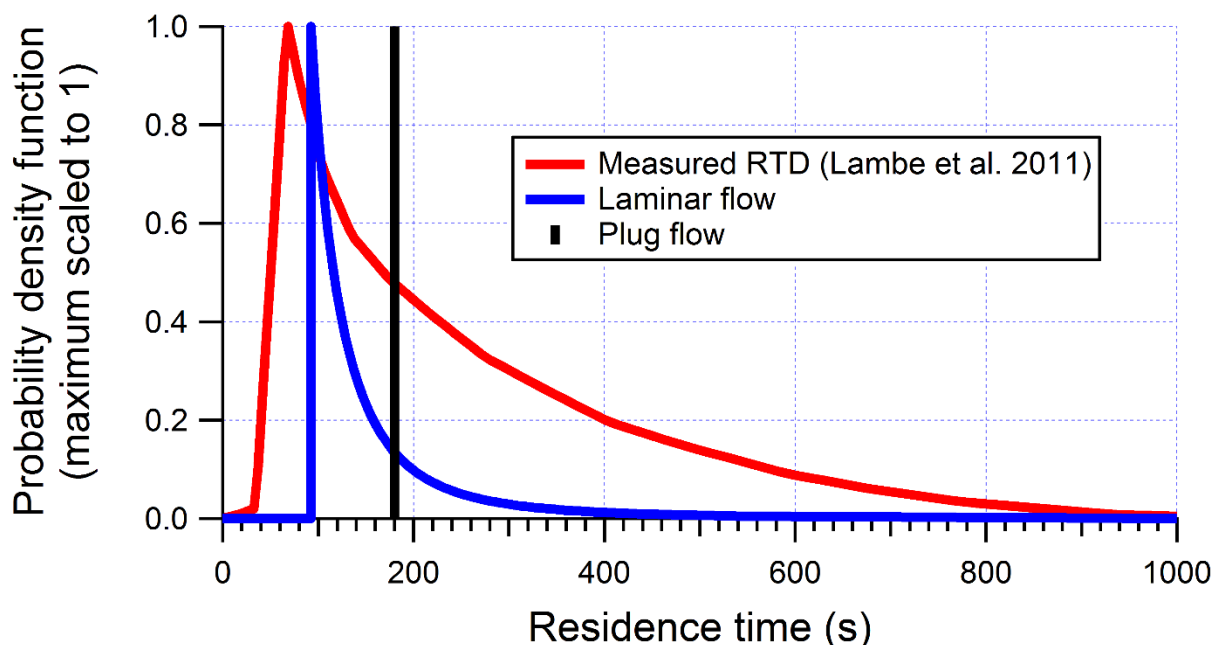


Figure S8. Residence time distribution (RTD) of plug and flows with the (average) residence time of 180 s and measured residence time distribution for the PAM (Lambe et al., 2011a), linearly scaled for the average residence time to be 180 s.

Figure 9 compares OH_{exp} for both RTDs and the plug flow case. The difference is quantified as the average ratio of OH_{exp} calculated from direct mathematical integration for each RTD case ($OH_{exp,RTD}^{MATH}$) to OH_{exp} in the plug-flow case ($OH_{exp,PF}$). The average ratios are, for OFR185, 0.83 and 1.75 for the laminar and Lambe RTDs, respectively, and, for OFR254 (including both OFR254-70 and OFR254-7), 0.86 and 1.42, respectively. The differences for the laminar RTD are smaller than the parametric uncertainty of the model due to uncertain chemistry parameters (Section 3.3). Considering all cases of OFR185 and OFR254 combined, all cases with the laminar RTD are within a factor of 2 from the plug-flow OH_{exp} , while a few percent of the Lambe RTD cases (under extreme conditions) are outside the range of a factor of 2 from $OH_{exp,PF}$. Within the datapoints for the Lambe RTD, those at lower OHR_{ext} are close to the corresponding plug-flow points, in agreement with Li et al. (2015). At very high OHR_{ext} (1000 s^{-1}), and in particular, at high H_2O and UV in OFR185, the deviations between the Lambe-RTD and plug-flow OH_{exp} can be larger (Fig. S9).

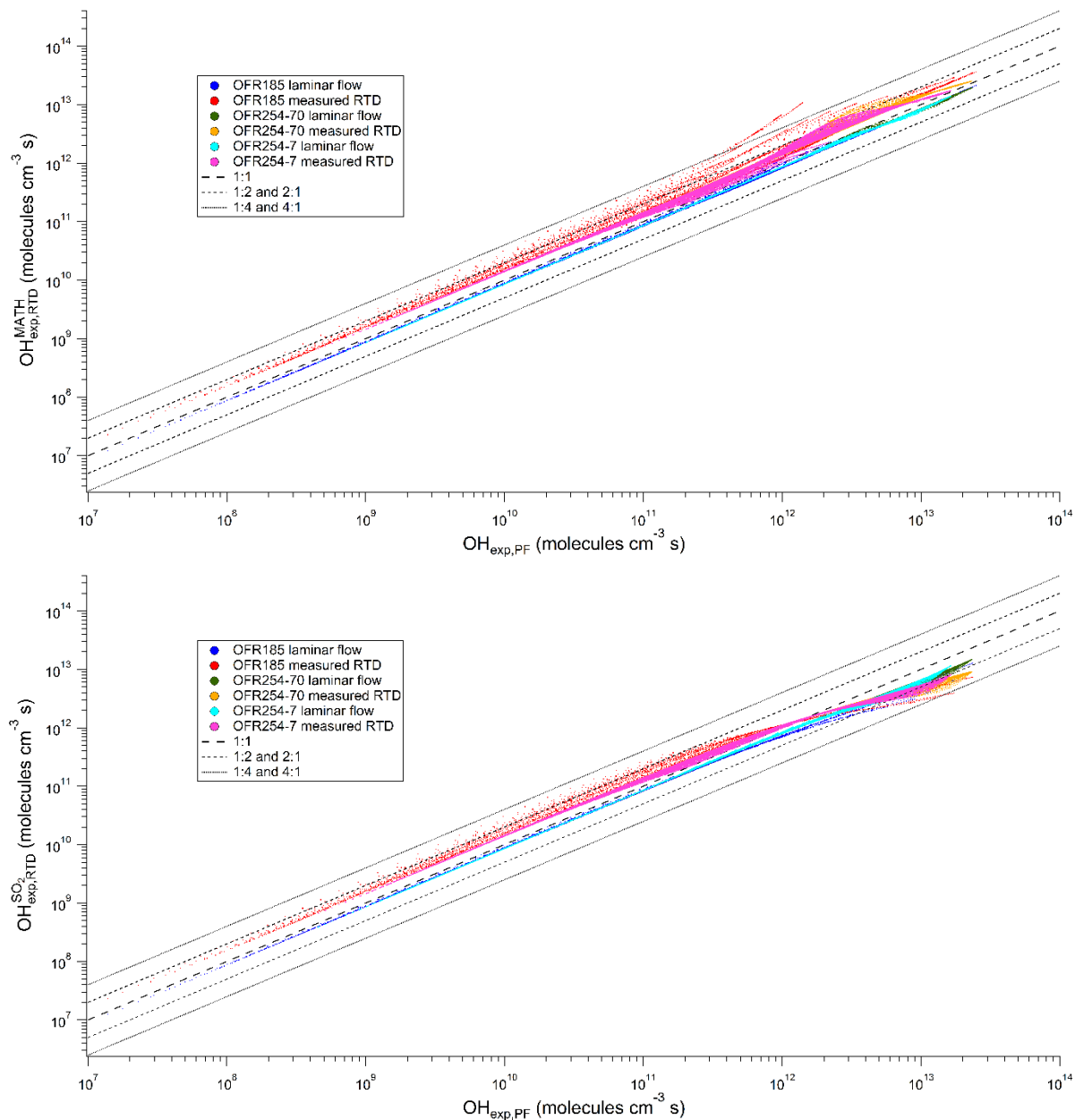


Figure 9. OH exposures calculated from direct integration ($\text{OH}_{\text{exp,RTD}}^{\text{MATH}}$, upper) and estimated from SO_2 decay ($\text{OH}_{\text{exp,RTD}}^{\text{SO}_2}$, lower) for the models with residence time distributions vs. those for the plug-flow model ($\text{OH}_{\text{exp,PF}}$). Note that for the plug-flow model both OH_{exp} definitions (MATH and SO_2) always have the same value, and thus that superscript is not used). The 1:1, 1:2, 2:1, 1:4 and 4:1 lines are also shown for comparison. For each type of RTD, 3600 (2700), 28800 (27900), and 28800 (27900) datapoints are shown in the upper (lower) panel for OFR185, OFR254-70, and OFR254-7, respectively.

In the cases of low OHR_{ext} , the generally small differences can be explained by the fact that OH reaches steady state very quickly (Li et al., 2015). Once this steady state is

reached, OH does not vary substantially with reaction time under most conditions (Fig. S10), since the OH production and consumption rates are roughly balanced. If OH remains roughly constant during the residence time, OH_{exp} varies linearly with residence time. Thus under these conditions $OH_{exp,PF}$ should be close to the average $OH_{exp,RTD}$ for any RTD. However, at high UV and very high OHR_{ext} , the following two conditions are simultaneously met: i) OHR_{ext} plays a dominant role in suppressing OH; ii) the consumption of the external OH reactant is substantial (Fig. S10). In this case, OH significantly increases as the external OH reactant is consumed. This causes $OH_{exp,RTD}^{MATH}$ to depend non-linearly on residence time. The Lambe RTD has a large portion at residence times much longer than the average value (>350 s), when almost all external OH reactant is destroyed and OH is approximately an order of magnitude higher than at the average residence time (180 s). This results in higher average $OH_{exp,RTD}^{MATH}$ with the measured RTD than $OH_{exp,PF}$ in OFR185. By contrast, the laminar RTD only has a very minor fraction at residence times >350 s, and hence OH_{exp} in good agreement with the plug-flow results is observed even at high H_2O , high UV, and very high OHR_{ext} .

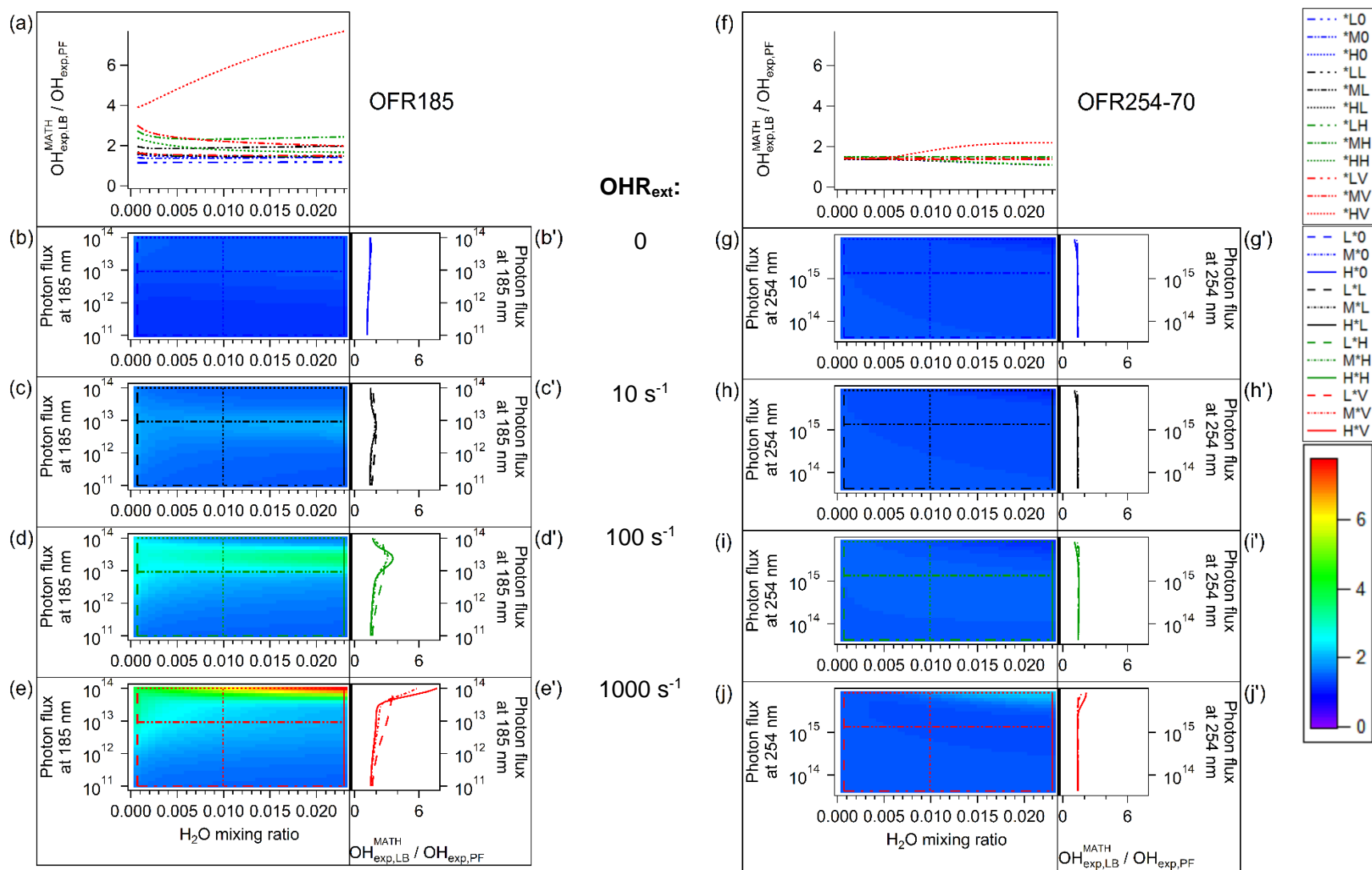


Figure S9. Dependence of the ratios of OH exposure calculated from direct integration in the model with measured residence time distribution (Lambe et al., 2011a) ($\text{OH}_{\text{exp,RTD}}^{\text{MATH}}$) to that in the plug-flow model ($\text{OH}_{\text{exp,PF}}$) in OFR185 and OFR254-70 on H_2O and UV, for OHR_{ext} of (b, g) 0, (c, h) 10, (d, i) 100, and (e, j) 1000 s^{-1} . (a, f) and (b'–j') are the line plots of these

ratios in several typical cases. These cases are denoted in the image plots (b–j) by horizontal or vertical lines of the same color and pattern as in the line plots.

In detail, the cut lines are in blue, black, dark green, and red in the plots for the cases of 0, low, high, and very high external OH reactivity, respectively. Vertical dashed, dash-dot, and solid lines mark low, medium, and high photon fluxes, respectively (first legend box). Horizontal sparse-dash-dot-dot, dash-dot-dot, and dotted lines mark low, medium, and high water mixing ratios, respectively (second legend box). Refer to Table 1 for more details on case labels. The color scale corresponds to all image plots.

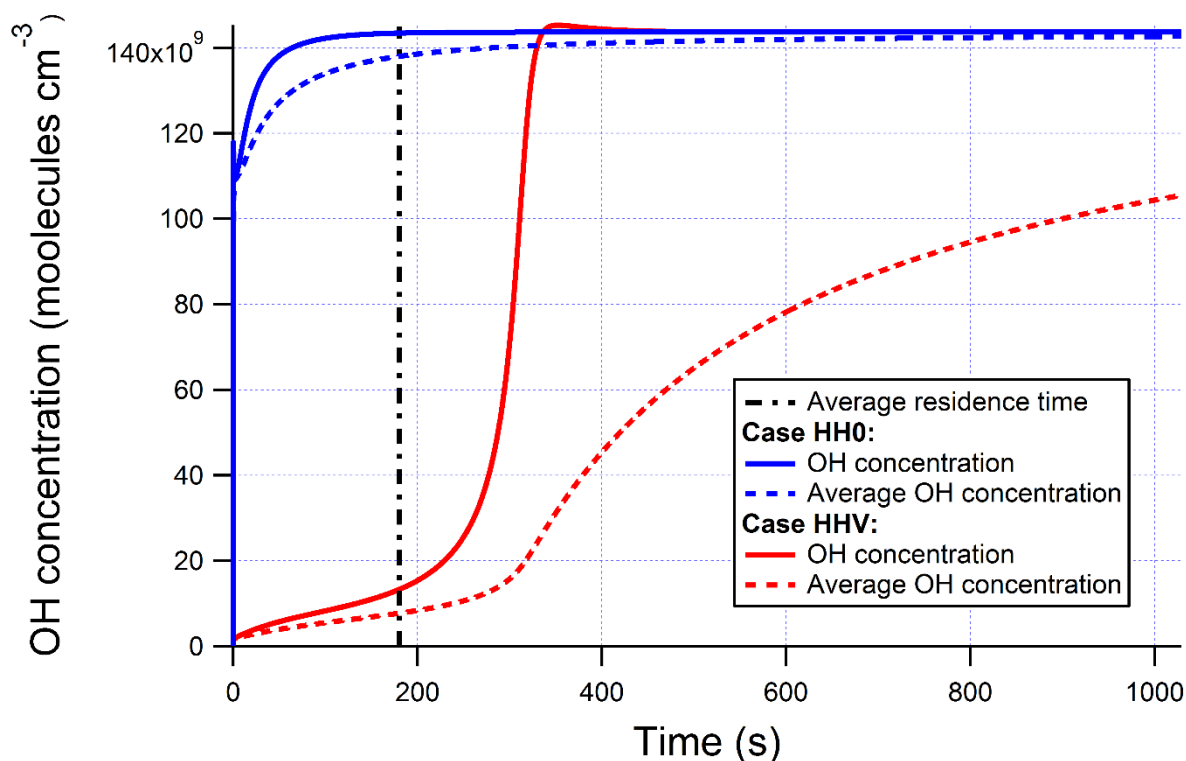


Figure S10. Instantaneous OH concentration vs. residence time in the reactor for Cases HH0 ($\text{OHR}_{\text{ext}} = 0$) and HHV ($\text{OHR}_{\text{ext}} = 1000 \text{ s}^{-1}$) in OFR185. For each case, average OH concentration over the elapsed reaction time is also shown. All curves (both instantaneous and integrated averages) are for individual air parcels and thus independent of model flow distributions.

Note that the differences between the plug-flow and Lambe-RTD $\text{OH}_{\text{exp}}^{\text{MATH}}$ for OFR185 at high H_2O , UV, and OHR_{ext} does *not* imply a poor performance of the plug-flow model. During the residence time $>350 \text{ s}$, OH is ~ 10 times higher than at the average residence time in Case HHV. However, at the same time, the external OH reactant is almost completely destroyed so that OH_{exp} in this period of time is irrelevant in terms of chemical processing of the external OH reactant. The ultimate goal of using OFRs is to oxidize external OH reactants (e.g., VOCs) rapidly. Therefore, in the case of a large part of OH_{exp} not being used for external OH reactant oxidation, it is better to consider the OH_{exp} that accounts for the external OH reactant oxidation rather than the total $\text{OH}_{\text{exp,RTD}}^{\text{MATH}}$. Therefore, we compare OH_{exp} estimated from the decay of an external OH reactant (SO_2 in this study, i.e. the experimental observable of the ratio of exit to intake concentration) calculated using the models with RTD ($\text{OH}_{\text{exp,RTD}}^{\text{SO}_2}$) to that in the plug-flow model (which is mathematically identical to $\text{OH}_{\text{exp,PF}}$) (Fig. 9b). Both types of OH_{exp} also compare generally well. Almost all cases of laminar RTD are within a factor of 2 of plug flow (Fig. S11), and the Lambe RTD cases deviating from $\text{OH}_{\text{exp,PF}}$ by a factor >2 are only a few percent (Table S1).

With both $\text{OH}_{\text{exp,RTD}}^{\text{MATH}}$ and $\text{OH}_{\text{exp,RTD}}^{\text{SO}_2}$ introduced, the difference between them can be assessed. In no case is the former smaller than the latter (Figs. 10 and S12). When OH_{exp} is low, both types of OH_{exp} tend to be identical, while $\text{OH}_{\text{exp,RTD}}^{\text{SO}_2}$ becomes significantly lower than $\text{OH}_{\text{exp,RTD}}^{\text{MATH}}$ when SO_2 is significantly consumed by OH (at $\text{OH}_{\text{exp}} > 10^{11}$ molecules $\text{cm}^{-3} \text{ s}$). For example, when half SO_2 is consumed, $\text{OH}_{\text{exp,RTD}}^{\text{SO}_2}$ (LB stands for the Lambe RTD) in OFR185 is ~30–70% lower than $\text{OH}_{\text{exp,RTD}}^{\text{MATH}}$. If SO_2 is nearly completely destroyed, $\text{OH}_{\text{exp,RTD}}^{\text{SO}_2}$ can be >5 times lower than $\text{OH}_{\text{exp,RTD}}^{\text{MATH}}$. The reason why significant SO_2 consumption can make a difference is that both the laminar and Lambe RTDs have a large portion of the flow with shorter-than-the-average residence time, which results in some parcels of air to passing through the reactor with little SO_2 reacting with OH, despite the large average OH_{exp} for the reactor. In the case of significant SO_2 consumption, the consumed SO_2 is also significantly less than that calculated from $\text{OH}_{\text{exp,RTD}}^{\text{MATH}}$. As a result, $\text{OH}_{\text{exp,RTD}}^{\text{SO}_2}$, estimated from consumed SO_2 , is lower than $\text{OH}_{\text{exp,RTD}}^{\text{MATH}}$. This suggests that $\text{OH}_{\text{exp,RTD}}^{\text{MATH}}$ may be significantly underestimated using a tracer in the OFR. On the other hand, $\text{OH}_{\text{exp,RTD}}^{\text{MATH}}$ may not be an appropriate measure of the photochemical aging of precursors since much of the periods that some air experiences high exposures may have little overlap with the presence of the precursors. Although we believe that SO_2 is generally a better surrogate for OHR_{ext} decay than primary VOCs as discussed above, using SO_2 as a surrogate is still a source of uncertainty. For this reason, for the most accurate estimation of photochemical aging relevant to a given OFR study, we recommend using the species under study to estimate it when possible, rather than using an additional tracer with very different lifetime as in some literature studies.

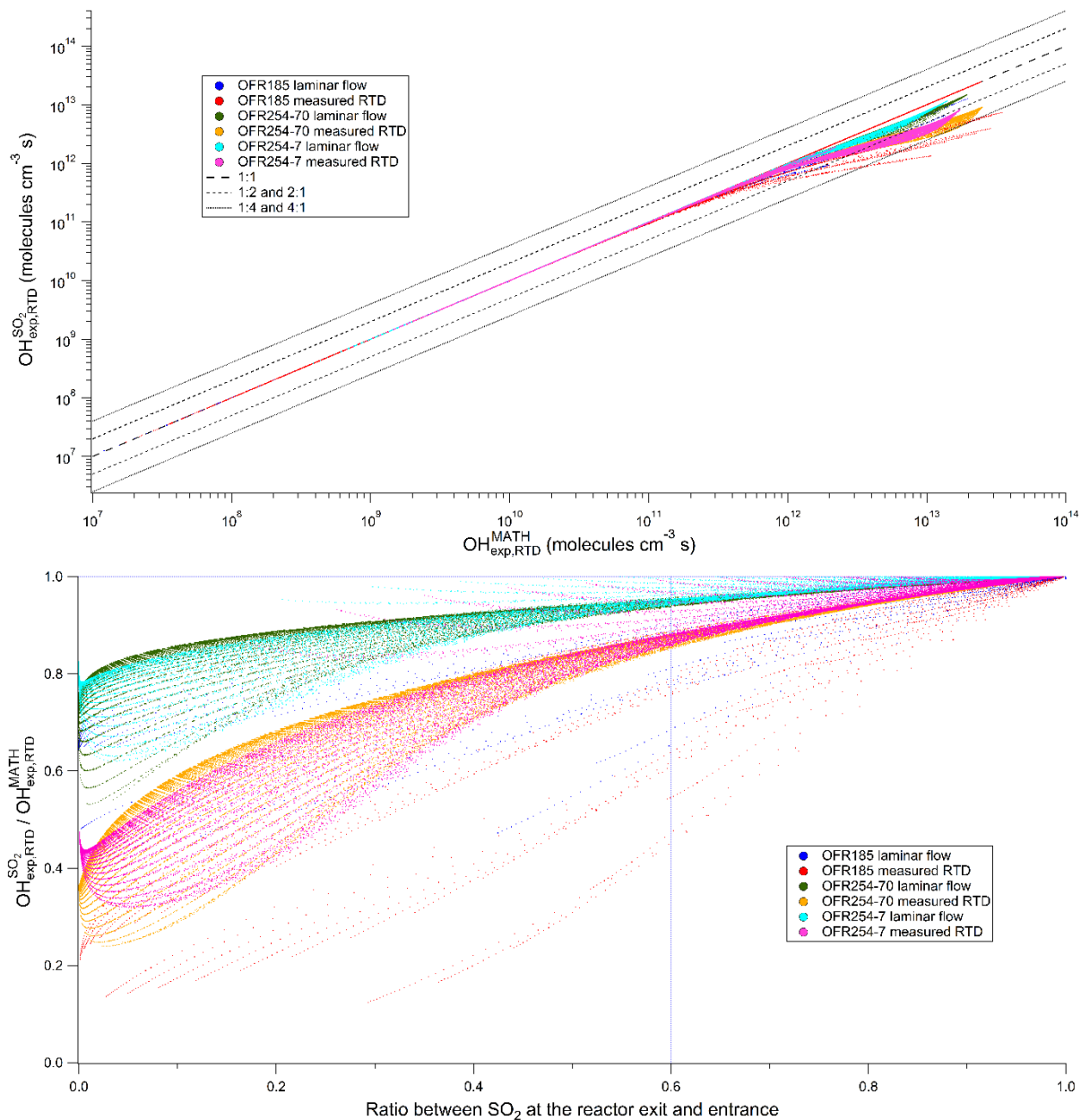


Figure 10. (upper) OH exposures estimated from SO₂ decay in the models with residence time distributions ($\text{OH}_{\text{exp,RTD}}^{\text{SO}_2}$) vs. those calculated from direct integration for the models with residence time distributions ($\text{OH}_{\text{exp,RTD}}^{\text{MATH}}$). The 1:1, 1:2, 2:1, 1:4 and 4:1 lines are also shown for comparison. (lower) Ratios between the two types of OH exposures as a function of the fractional consumption of SO₂ in the reactor. For each type of RTD, 2700, 27900, and 27900 datapoints are shown for OFR185, OFR254-70, and OFR254-7, respectively.

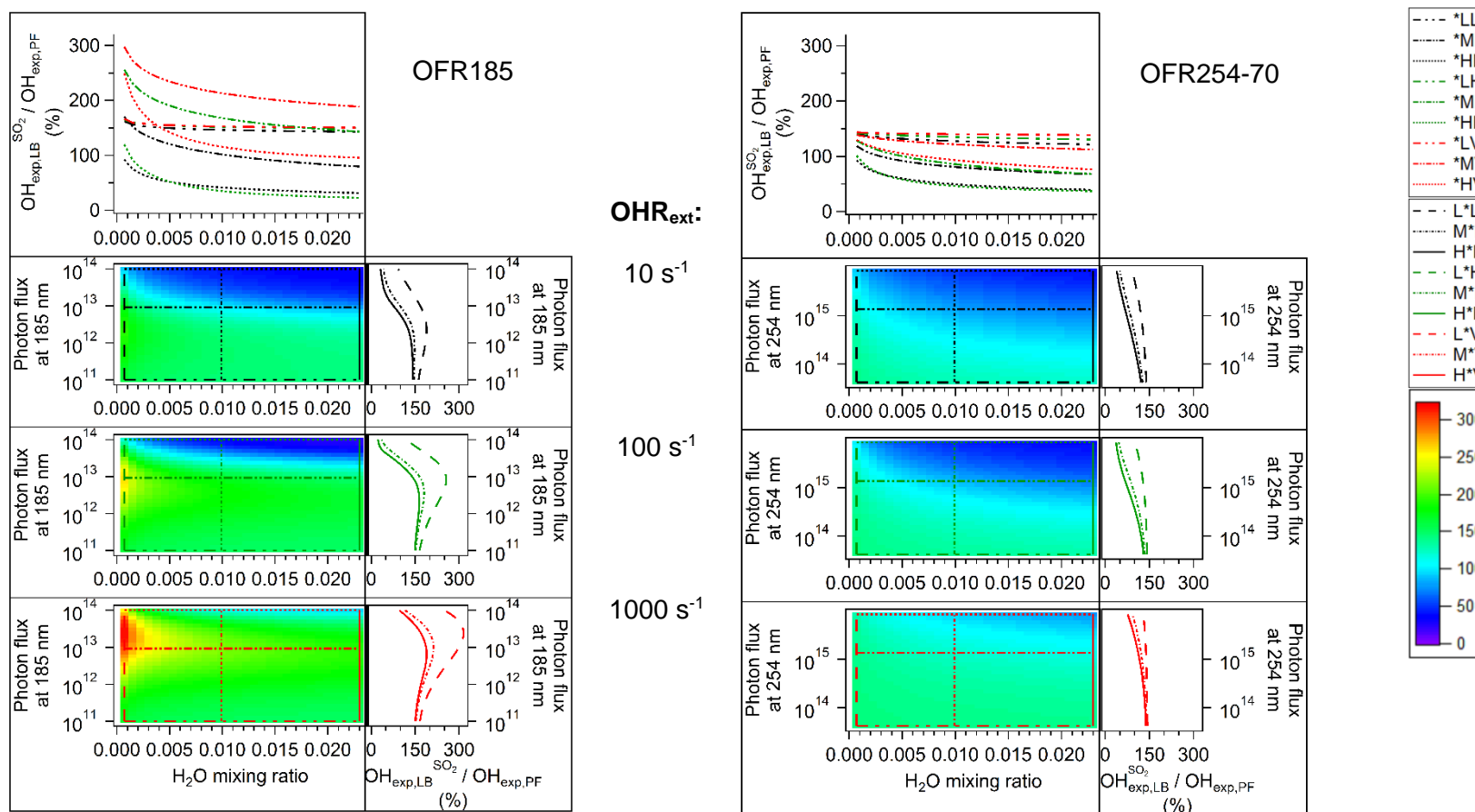


Figure S11. Percentage of OH exposure estimated from SO₂ decay in the model with the Lambe et al. (2011a) residence time distribution (OH_{exp,SO₂}) to OH exposure in the plug-flow model (OH_{exp,PF}) vs. the same parameters and in the same format as Fig. 2.

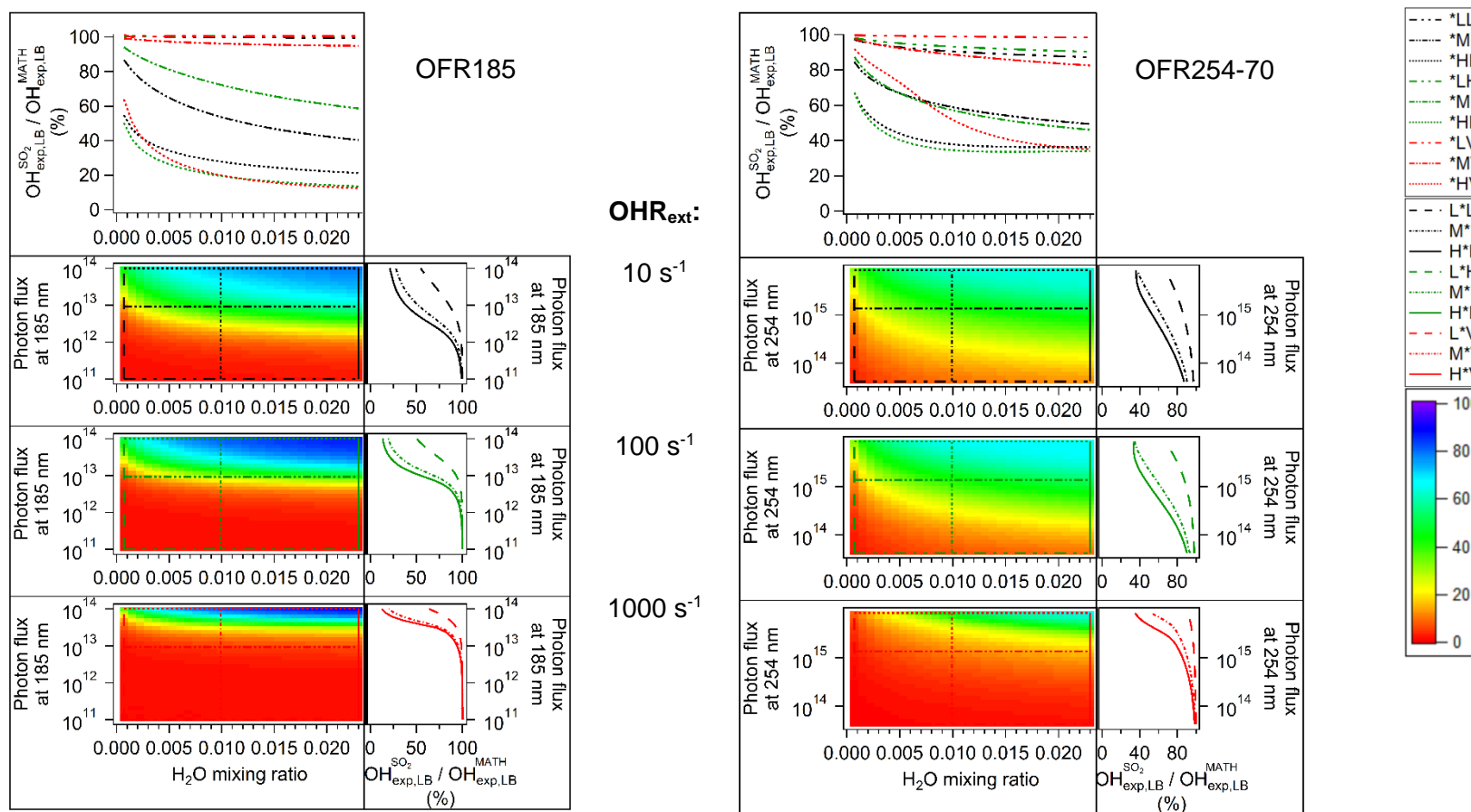


Figure S12. Percentage of OH exposure estimated from SO₂ decay in the model with the Lambe et al. (2011a) residence time distribution ($\text{OH}_{\text{exp, LB}}^{\text{SO}_2}$) to that calculated from direct integration in the same model ($\text{OH}_{\text{exp, LB}}^{\text{MATH}}$) vs. the same parameters and in the same format as Fig. 2.

Table S1. Statistics of the ratio among OH exposures calculated in the models with the laminar and Lambe et al. (2011a) residence time distributions ($\text{OH}_{\text{exp,RTD}}^{\text{MATH}}$), estimated from SO₂ decay in the same model ($\text{OH}_{\text{exp,RTD}}^{\text{SO}_2}$), and calculated in the plug-flow model ($\text{OH}_{\text{exp,PF}}$). The geometric mean, uncertainty factor, and percentage of outlier cases (>2 or <1/2) are shown for OFR185, OFR254-70, and OFR254-7. Statistics for all cases with the laminar and Lambe et al. residence time distributions are also reported.

OFR type	$\text{OH}_{\text{exp,RTD}}^{\text{MATH}} / \text{OH}_{\text{exp,PF}}$			$\text{OH}_{\text{exp,RTD}}^{\text{SO}_2} / \text{OH}_{\text{exp,PF}}$			$\text{OH}_{\text{exp,RTD}}^{\text{SO}_2} / \text{OH}_{\text{exp,RTD}}^{\text{MATH}}$		
	Geom. Mean	Uncert. factor	Outlier cases (%)	Geom. mean	Uncert. factor	Outlier cases (%)	Geom. mean	Uncert. factor	Outlier cases (%)
OFR185 Laminar	0.86	1.06	0	0.79	1.19	2	0.90	1.19	2
OFR185 Lambe	1.75	1.35	23	1.35	1.58	13	0.70	1.67	22
OFR254-70 Laminar	0.86	1.02	0	0.76	1.11	0	0.89	1.11	0
OFR254-70 Lambe	1.42	1.09	0	0.95	1.40	6	0.67	1.39	21
OFR254-7 Laminar	0.86	1.02	0	0.81	1.10	0	0.94	1.10	0
OFR254-7 Lambe	1.41	1.10	0	1.12	1.34	2	0.80	1.34	12
All Cases Laminar	0.86	1.04	0	0.79	1.14	1	0.91	1.14	1
All Cases Lambe	1.52	1.24	8	1.13	1.49	7	0.72	1.49	15

We have made additional changes to the manuscript text to reflect the addition of the new text and figures on the non-plug-flow cases. We have added text to the abstract (P3884/L27) stating:

“OH_{exp} calculated from direct integration and estimated from SO₂ decay in the model with laminar and measured residence time distributions (RTDs) are generally within a factor of 2 from the plug-flow OH_{exp}. However, in the models with RTDs, OH_{exp} estimated from SO₂ is systematically lower than directly integrated OH_{exp} in the case of significant SO₂ consumption. We thus recommended using OH_{exp} estimated from the decay of the species under study when possible, to obtain the most appropriate information on photochemical aging in the OFR.”

The following text has been added to the conclusions section (P3913/L15):

“We also investigated the effect of non-plug flow. Compared to the plug-flow model, applying the residence time distributions of laminar flow and that measured by Lambe et al. (2011a) results in OH_{exp} generally within a factor 2. However, OH_{exp} calculated from direct integration in the models with residence time distributions is significantly higher than that estimated from SO₂ decay in the same model, when SO₂ is significantly consumed. Considering various rate constants of reactions of precursors with OH, we thus recommend using OH_{exp} estimated from the decay of species under study, if possible, as the appropriate measure of photochemical aging in the OFR.”

We have also removed “**plug flow**” from P3900/L25.

R1.3) Figures 2-4, 6-7 are multi-paneled, extremely complex, small font and of low image quality. I would highly recommend removing many of the panels to simplify the figure presentation. The panels that are removed can be placed in the supporting information. For example it doesn't seem necessary to include 3 OH reactivity panels (perhaps only 0 and 100 s⁻¹). It is simply too difficult for the reader to wade through these complex figures in any detail as she is reading the paper. At the very least higher resolution images and bigger fonts are needed.

We agree that figures in the format similar to Fig. 2 are complex and that their image quality could be improved. However, removing the panels for 10 s⁻¹ may make some trends unclear, e.g., in Fig. S2 in the AMTD paper, the panels for 10 s⁻¹, where OHR_{int} and OHR_{ext} are comparable, are crucial to illustrate the gradual transition of dominance from OHR_{int} to OHR_{ext}. Thus, we have made an effort to increase the image quality, but prefer to keep the multi-paneled format. In addition, we also made additional changes to the figures as suggested by Referee #3 (see response to R3.7).

R1.4) I would also recommend a table of symbols and their definitions to make it easier for the reader to understand the short hand nomenclature used throughout the manuscript.

We have created the following table of short-hand nomenclature and added it to the end of the manuscript text.

OFR	oxidation flow reactor
OFR185	oxidation flow reactor using both 185 and 254 nm light
OFR254	oxidation flow reactor using 254 nm light only
OFR254-X	OFR254 with X ppm O₃ initially injected
OH_{exp}	OH exposure
H₂O	water mixing ratio
UV	UV light intensity
O₃	O₃ concentration
OHR	OH reactivity
OHR_{tot}	total OH reactivity
OHR_{int}	internal OH reactivity (due to O₃, HO₂, OH, and H₂O₂)
OHR_{ext}	external OH reactivity
OHR_{O3}	OH reactivity from O₃ only
VOC	volatile organic compound
SOA	secondary organic aerosol
RTD	residence time distribution
OH_{exp,PF}	OH exposure in the plug-flow model
OH_{exp,RTD}^{MATH}	OH exposure calculated from direct integration in the models with residence time distribution
OH_{exp,LB}^{MATH}	OH exposure calculated from direct integration in the models with the Lambe et al. (2011a) residence time distribution
OH_{exp,RTD}^{SO2}	OH exposure estimated from SO₂ decay in the models with residence time distribution
OH_{exp,LB}^{SO2}	OH exposure estimated from SO₂ decay in the models with the Lambe et al. (2011a) residence time distribution
rOH_{exp}	Ratio of remaining OH after suppression
O_{3,in}	O₃ concentration at the reactor entrance
O_{3,out}	O₃ concentration at the reactor exit
rO₃	ratio of O_{3,out} to O_{3,in}

Anonymous Referee #3

The authors present a model of the chemistry that occurs within their oxidation flow reactor. This is an extension over previous work published by some of the co-authors. They discuss, importantly, the influence of OH suppression within the OFR, which complicates the relationship between light intensity and [OH]. This is an interesting work, although I have some concerns regarding the extent to which the model accurately simulates the system conditions, in particular the flow dynamics and timescales involved (the simulations assume plug flow, which is not correct for the OFR). It may very well be that this has no bearing on the conclusions, but as the conclusions are made quite strongly it is up to the authors to demonstrate that it is not an important limitation. That said, the authors do provide some relationships between various controlling factors ([O₃], [H₂O], UV) as well as some general insights into OFR behavior that will be of use to the burgeoning community of OFR users. I believe that this paper is certainly publishable once the address the comments provided here, as well as those of the other reviewers and commentators.

R3.1) P3887/L9: It would be clearer to simply give an equation for the OHR_{ext} than the text that is written

We have modified the text in P3887/L9 to read:

“OHR_{ext} = $\sum_i k_i [R_i]$, where k_i and $[R_i]$ are the rate constant with OH and the concentration of the i^{th} OH-consuming reactant in the system. This calculation excludes “internal” OH reactants, namely OH, HO₂, O₃, and H₂O₂.”

R3.2) Flow: The authors assume plug flow. However, as discussed by Lambe in his comment, the flow in the OFR is not plug flow, but instead is more similar to a CSFTR, leading to a distribution of lifetimes and exposures. This would seem to me to be a major potential limitation of the model that is not addressed. I believe that the authors need to address issues related to the flow conditions of their OFR and how these would influence their conclusions. The equations describing the flow conditions in a CSFTR are known (Mason and Piret, 1950). The authors do note (p3891) that the assumption of plug flow should be the focus of future studies. However, given statements such as at the end of the abstract (“This study contributes to establishing a firm and systematic understanding of the gas-phase HO_x and O_x chemistry in these reactors, and enables better experiment planning and interpretation as well as improved design of future reactors.”) it would seem that consideration of this effect in particular is especially important in the current context. I believe that the authors should carefully consider the questions posed by Lambe and co-workers in his comment.

See response to comment R1.2.

R3.3) P3890: I find the statement “although SO₂ is consumed by OH much more slowly than most primary VOCs, it is actually more realistic in terms of the decrease of total OH reactivity than using only the first generation reaction of a VOC, since the latter ignores the continuing reactivity of the products.” to be somewhat unclear in terms of how specifically using SO₂

actually captures the influence of “continuing reactivity of the products” that are missed if primary VOCs had been used. Is this simply saying that because SO₂ products do not react with OH, there are fewer complications?

We made this statement in terms the OHR_{ext} decay, in other words, the effective OHR_{ext} during the residence time.

We have modified the text on P3890/L8 to clarify this point:

“Although SO₂ is consumed by OH much more slowly than most primary VOCs, it is actually more realistic in terms of the decrease of total OH reactivity than using only the first generation reaction of a VOC. If we only consider the primary oxidation of VOCs, OHR_{ext}, due to most VOCs should very quickly decrease to ~0, then has no effect during most of the residence time, leading to low effective OHR_{ext}. Actually, products of primary VOC oxidation can undergo further oxidation acting as external OH reactants. As a result, the decay of OHR_{ext} due to total VOCs is usually much slower than that due to primary VOCs. We thus believe that SO₂ can better capture the features of real OHR_{ext} decay and effective OHR_{ext}.”

R3.4) P3894: Looking at Fig. 1, I am not certain the statement “Note that the production, consumption, and interconversion of HO_x have average rates on the same order of magnitude within each type of OFR.” Is fully justified. For example, the conversion flux given for O₃ going to OH is 8.3 for OFR185 but 171.2 for OFR254-70, which is a factor of nearly 20 different.

The sentence quoted by the reviewer already states that this is valid only “*within each type of OFR*”. Therefore, fluxes for OFR185 cannot be compared to those for OFR254-70. The conversion flux given for O₃ going to OH in OFR254-70, 171.2x10¹⁰ molecules cm⁻³ s⁻¹, can be compared to, for example, those from HO₂ to H₂O and from H₂O₂ to HO₂ (51.5 and 28.9x10¹⁰ molecules cm⁻³ s⁻¹, respectively), which are both within an order of magnitude of 171.2x10¹⁰ molecules cm⁻³ s⁻¹.

R3.5) I find the statement(s) on P3895 regarding the sensitivity of OH_{exp} to the inputs to be somewhat ambiguous/difficult to understand specifically what is meant. I suggest that the authors clarify.

We have modified the text in P3895/L23 to read:

“OH_{exp} in both types of OFRs are similarly sensitive to the inputs (H₂O, UV, and OHR_{ext}) under the conditions of higher H₂O, UV, and lower OHR_{ext}. OFR185 is more sensitive to the inputs than OFR254-70 at lower H₂O and UV and high OHR_{ext}.”

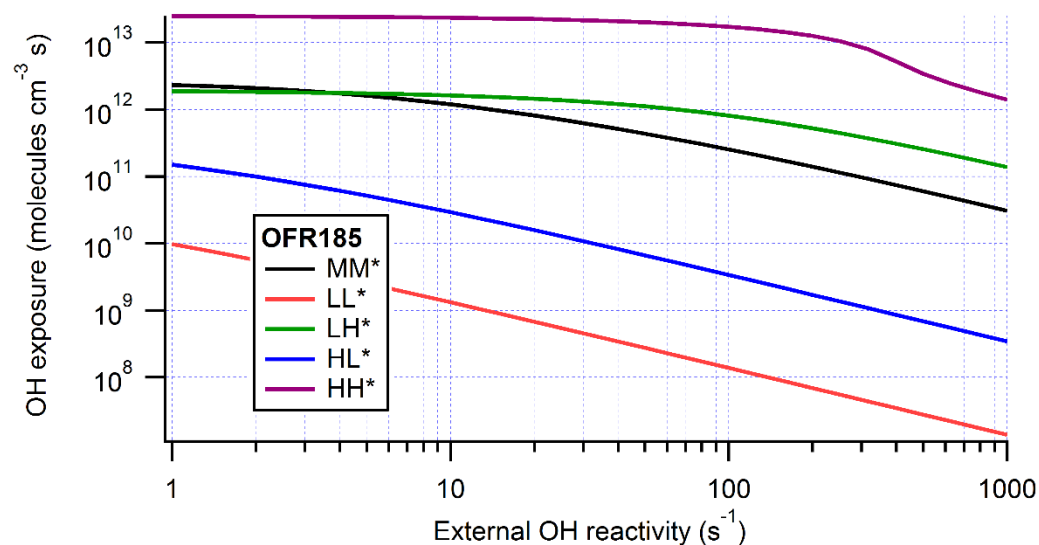
R3.6) An entire section is pretty much written around a supplemental figure (Fig. S2), which suggests to me that this figure belongs in the main paper.

In response to this comment we have moved this figure to the main paper.

R3.7) It seems to me that it would be simpler to include Figs. S5-S9 in Figs. 2-4 and the other associated figures. Is there a particular reason that the $\text{OHR}_{\text{ext}} = 1000 \text{ 1/s}$ case was not included in the main graphs? If not, then I suggest that it is included. Alternatively, or perhaps in addition to, it seems that since the role of OHR_{ext} is a relatively major focus of this paper, it would be helpful to have some figure showing the dependence of e.g. OH_{exp} vs. OHR_{ext} for some fixed H_2O and UV. The authors could potentially have one axis as OHR_{ext} with complementary axes for equivalent concentrations of different reacting species (e.g. SO_2 , NO , some favorite VOC) so as to give an idea of the concentration ranges over which one should be concerned. This would ultimately be more useful to experimentalists, who can easily control the concentrations (at least for things that are not naturally in the atmosphere, but at least for lab experiments) but for whom OHR_{ext} is a somewhat more abstract experimental variable.

The original reason to keep the $\text{OHR}_{\text{ext}} = 1000 \text{ s}^{-1}$ panels in the Supp. Info was to increase figure size in the AMTD page format, to increase readability. To address this comment we have combined Figs. S5–S9 in the AMTD version with the corresponding figures in the main paper, and removed them from the Supp. Info. Similarly we have also combined Fig. S12 in the AMTD paper with Fig. 7 in the AMTD paper. We will make sure that the figures are reproduced in as large a format as possible in the final AMT version, for readability.

In response to the 2nd part of the comment about more clearly showing the trends vs. OHR_{ext} and the relationship between OHR_{ext} and mixing ratio for different reactants, we have added the following figures to the supplementary information:



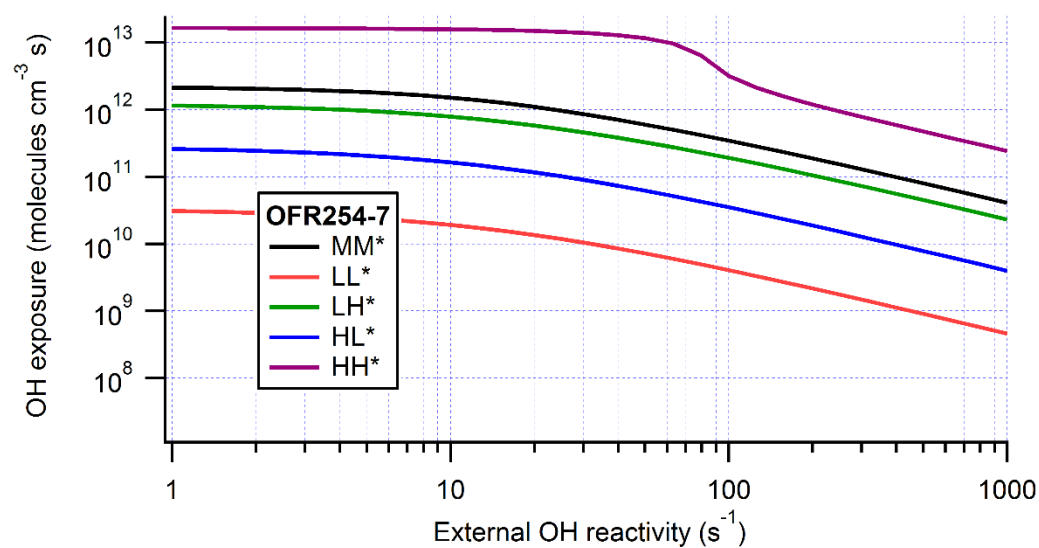
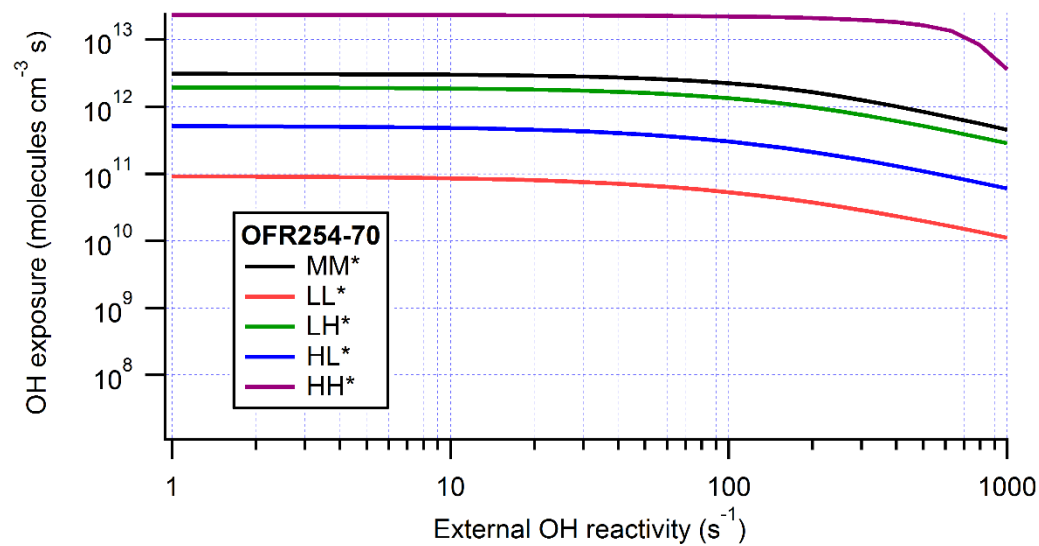


Fig. S4. OH exposures in typical cases of OFR185 (top), OFR254-70 (middle), and OFR254-7 (bottom) as a function of external OH reactivity.

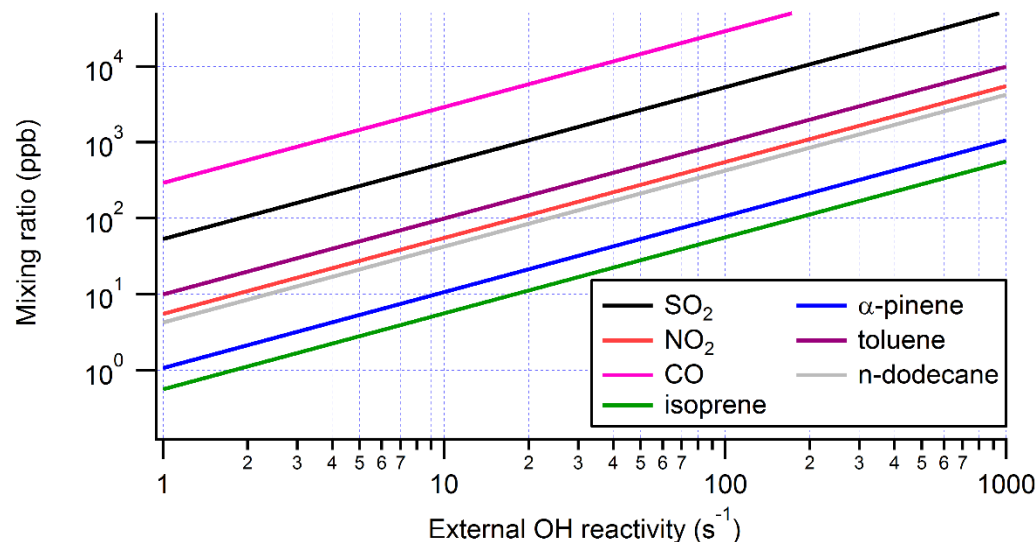


Fig. S1. Volume mixing ratios of several external OH reactants corresponding to different external OH reactivities.

We also refer to Fig. S4 in P3898/L23 and L27 and to Fig. S1 in P3890/L5, respectively.

R3.8) It is somewhat unclear what is specifically meant by the statement at the end of P3899 that “Very high OHR_{ext} also results in much increased relative importance of non-OH driven reactions in both OFRs, which will be addressed in future work.” What reactions are being referred to?

We have since submitted Peng et al. (2015b), which addresses the issue of non-OH driven reactions and is now published in ACPD. To briefly clarify this issue, we modify the text in P3899/L28 to read:

“Very high OHR_{ext} also results in much increased relative importance of non-OH driven reactions in both OFRs. Under those conditions, OH is heavily suppressed while other reactants that can consume some types of VOCs, e.g., 185 and 254 nm photons for aromatics and O_3 for alkenes, may not be significantly affected compared to moderate OHR_{ext} cases. Thus, those non-OH reactants may destroy comparable or larger amounts of VOCs than OH does at very high OHR_{ext} . This issue is investigated in detail in Peng et al. (2015).”

R3.9) For Fig. 5 and associated discussion, it should be noted that the lack of sensitivity (uncertainty) to the reaction rate of OH with some external species (e.g. SO_2 , VOC) is because these were exactly specified in the model and thus do not have uncertainty. In a real system, where the identities and relative abundances of all reacting species may not be known, uncertainty in the OHR_{ext} will also be important. This is sort of noted at the bottom of P3900, but it could be made clearer that this has the potential to be a major uncertainty.

We agree with this comment and modify text to P3901/L1:

“The uncertainties in comparing the model results to experiments are likely dominated by the simplifications introduced in the model (e.g., uniform radiation field and no wall effects), as well as by incomplete information about the experimental inputs (e.g. dependence of UV light output on ambient temperature and lamp age, quantification of OHR_{ext} from primary VOCs and their oxidation intermediates, limited knowledge of species entering the reactor in field studies, etc.)”

R3.10) P3901, Line 23: Technically, OH is produced by $\text{O}(1\text{D}) + \text{H}_2\text{O}$, not $\text{O}_3 + 254 \text{ nm}$, although of course the O_3 photolysis is the primary source of the $\text{O}(1\text{D})$.

Indeed OH is directly produced by $\text{O}(1\text{D}) + \text{H}_2\text{O}$. However, we do not think that “ $\text{O}_3 + 254 \text{ nm}$ ” would be confusing. However, for clarity, we have modified the text on P3894/L20 to read:

“Both reactors form primary OH from $\text{O}_3 + 254 \text{ nm}$ (via $\text{O}_3 + 254 \text{ nm} \rightarrow \text{O}_2 + \text{O}(1\text{D})$ and $\text{O}(1\text{D}) + \text{H}_2\text{O} \rightarrow 2\text{OH}$), while OFR185 produces 70% of its primary HO_x from $\text{H}_2\text{O} + 185 \text{ nm}$.”

R3.11) Figure 6: I find this figure could be clearer as to whether the authors are showing the “percentage of OH exposure” or the “Ratio of OH exposure to the base case”, as both are used (yet have different meanings). I believe they report only the “ratio”, in conflict with what is stated in the caption. Additionally, it is difficult to tell the upper limit of the color scale.

We have modified the caption of Fig. 7 (Fig. 6 in the AMTD paper) and added minor ticks to the color scale legend to more clearly show its upper values, as shown below:

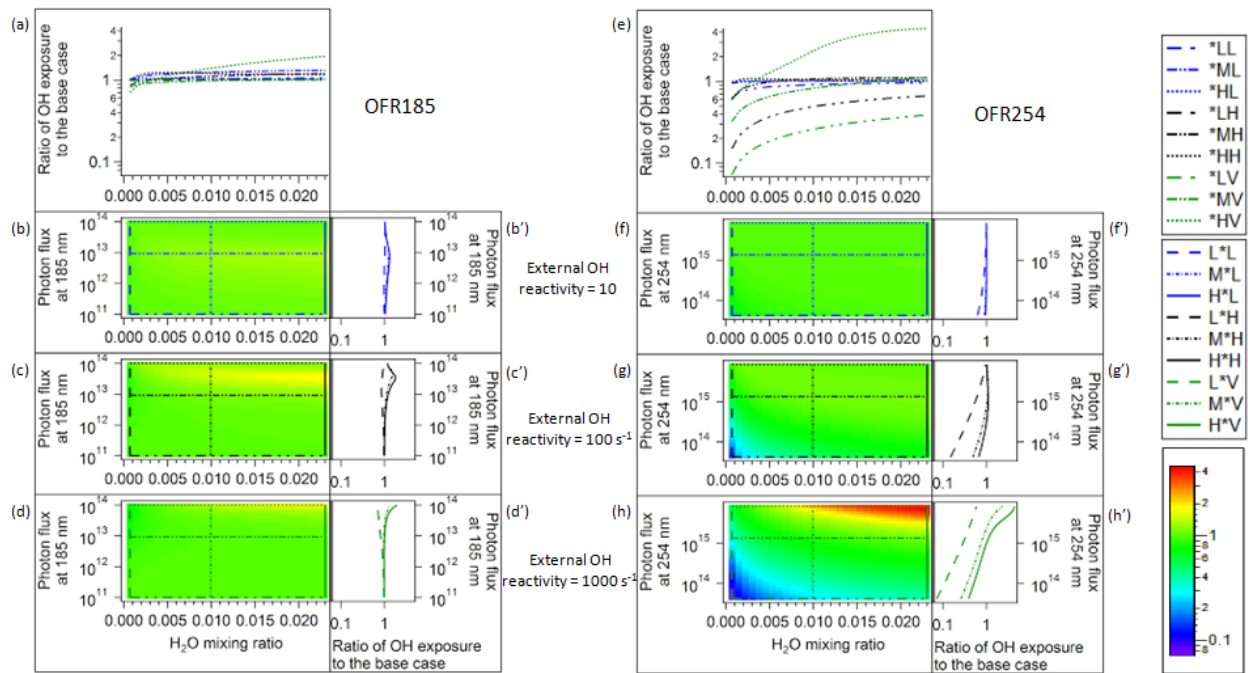


Figure 7. Ratio of OH exposure in the case of HO_x -destructive external OH reactivity (OHR_{ext}) to that in the base case (Fig. 2) vs. the same parameters and in the same format

as Fig. 2, but for the cases of low (10 s^{-1}), high (100 s^{-1}), and very high (1000 s^{-1}) external OH reactivity.

R3.12) Figs. 6, S10 and S11: The authors keep switching between percent changes and ratios. They should pick one and use it consistently. It is otherwise a potential point of confusion to the reader.

We do not think that using only one of percentage and ratio consistently for all Figs. 6, S10, and S11 in the AMTD version would be clearer. If ratios are close to 1, it is clearer to discuss percentages, as in Fig. S10 of the AMTD paper. However, in Figs. 6 and S11 of the AMTD paper, there are ratios more than an order of magnitude lower/higher than 1. Thus it is more appropriate to show ratios in those figures. Thus, we prefer to keep the quantities shown in those figures as they are.

R3.13) P3904/Fig. S11: I do not agree that the overall effect of replacing SO_2 with a collision rate limited reaction is “more dramatic”, in particular for the OFR254-70 case. In fact, the ratio there sits right around unity for nearly all conditions. Only very particular conditions lead to strong deviations. Of course, the behavior of OFR185 is much more complex.

We have modified the text to P3904/L15 to clarify this point:

“The effect of replacing SO_2 by a reactant with collision rate is more dramatic in OFR185 than for OFR254-70. OFR254 is more sensitive at lower input O_3 .”

R3.14) P3905, Line 17: The qualitative word “minor” should be removed, as 40-80% change might be considered more than “minor” by some. 80% is nearly an order of magnitude.

40–80% does not refer to a change but rather to the percentage of OH_{exp} in OFR254-7 relative to that in OFR254-70. Thus, this range means 20% to a factor of ~2 lower. This is substantially less than an order-of-magnitude, i.e., a factor of 10. Considering a 10 times lower O_3 concentration, this is not a large change. We have however changed the word “minor” to “relatively small” here.

For more clarity, we have modified the text in P3905/L15 to read:

“The ratio of OH_{exp} in OFR254-7 to that in OFR254-70 is shown in Fig. 8. At 0 OHR_{ext} (Fig. 8b, b’), OH_{exp} in OFR254-7 is ~40–80% of that in OFR254-70, despite a lower initial O_3 concentration by a factor of 10. This relatively small difference in OH_{exp} is due to both OH production and consumption that are slowed down simultaneously.”

R3.15) Fig. 8: It is not abundantly clear what “percentage of remaining OH after suppression” means. Is this some ratio to some base case? What is the “before suppression” case? When $\text{OHR}_{\text{ext}} = 0$?

We have modified the text on P3906/L24 to address this point:

“After that, the percentage of remaining OH after suppression (rOH_{exp} , i.e., the percentage of OH relative to that in the case with $OHR_{ext}=0$) exhibits a nearly exponential decrease with decreasing OHR_{O_3}/OHR_{ext} .”

Short Comment by Lambe et al.

SC.0) Peng et al. extends previous work by Li et al. (2015) in presenting a modeling analysis that is used to characterize radical chemistry in oxidation flow reactors (OFRs) using OH radicals produced from photolysis of radical precursors (O_2 , H_2O , O_3) at $\lambda = 185$ and/or 254 nm. The radical chemistry is systematically characterized as a function of UV irradiance and mixing ratios of O_3 and H_2O that are input to the OFR. Perturbations in the radical chemistry are additionally examined in the presence of added HO_x sinks such as NO_x and VOCs. These results are used to interpret previous OFR measurements and also to derive empirical OH exposure estimation equations.

Peng et al. addresses the need for improved characterization of OFRs as an emerging atmospheric measurement technique for providing inputs to chemistry and climate models. However, the analysis of VOC- and NO_x - induced perturbations to OFR radical chemistry is incomplete and is not supported by available measurements. Excluding this model/measurement comparison provides no context within which to evaluate the accuracy of the modeled OH suppression.

We strongly disagree that the modeling in this manuscript is not supported by measurements. Li et al. (2015) validated the model results for OH_{exp} using measurements of the decay of SO_2 and CO, as well as for output O_3 , over a wide range of conditions, and provided model / measurement comparisons (their Fig. 5, reproduced below). Measured and modeled OH_{exp} agreed well. We did already state this in our AMTD manuscript (P3887/L4): “The kinetic model that Li et al. (2015) developed compared well against measurements of OH exposure and O_3 concentration in laboratory calibration experiments and field studies using OFR185.” We thus did not see a reason to repeat that type of comparison in the current manuscript.

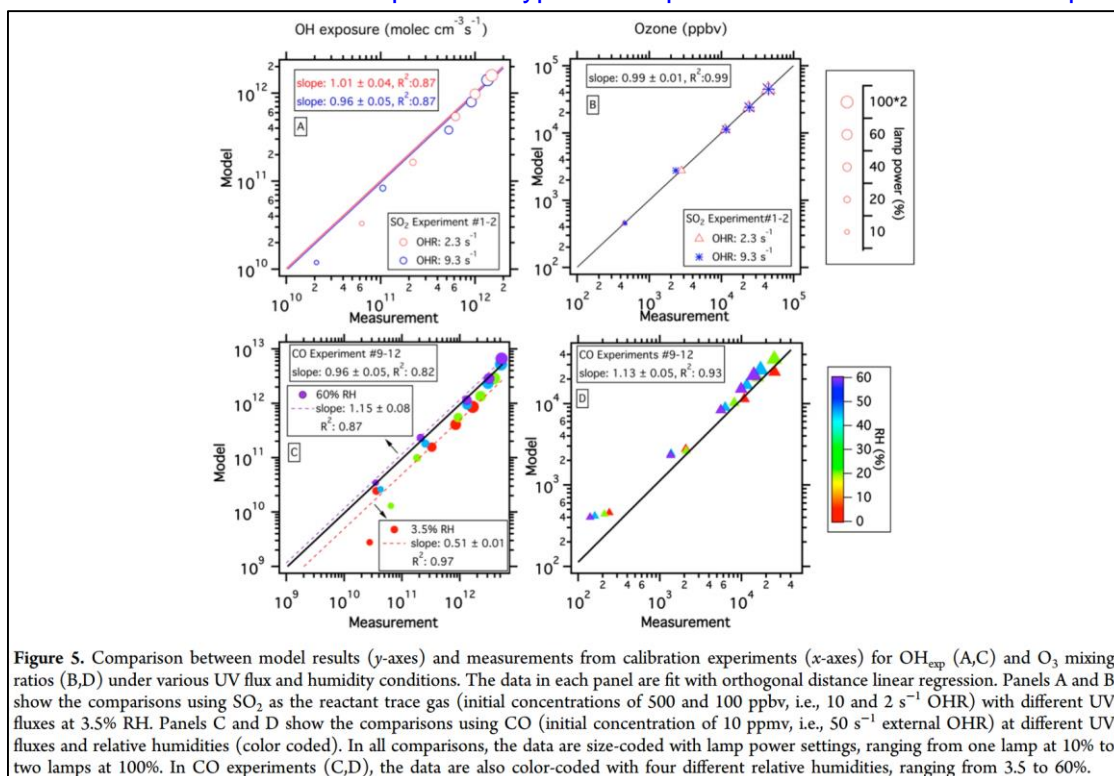


Figure 5. Comparison between model results (y-axes) and measurements from calibration experiments (x-axes) for OH_{exp} (A,C) and O_3 mixing ratios (B,D) under various UV flux and humidity conditions. The data in each panel are fit with orthogonal distance linear regression. Panels A and B show the comparisons using SO_2 as the reactant trace gas (initial concentrations of 500 and 100 ppbv, i.e., 10 and 2 s^{-1} OHR) with different UV fluxes at 3.5% RH. Panels C and D show the comparisons using CO (initial concentration of 10 ppmv, i.e., 50 s^{-1} external OHR) at different UV fluxes and relative humidities (color coded). In all comparisons, the data are size-coded with lamp power settings, ranging from one lamp at 10% to two lamps at 100%. In CO experiments (C,D), the data are also color-coded with four different relative humidities, ranging from 3.5 to 60%.

The measure of OH suppression used in our paper, i.e. the percentage of remaining OH after suppression, is just a ratio between OH_{exp} with and without OHR_{ext} . Validating the model results of OH_{exp} is thus conceptually the same as validating the results of OH suppression. Thus the previous validation of the model published by Li et al. (2015) supports the validity of the model OH suppression.

In terms of other contributions to the model uncertainty, in the AMTD version we had already investigated the uncertainty of the model OH_{exp} due to uncertain kinetic parameters (see Section 3.3). In response to comments R1.2, R3.2, and SC.3 we have investigated the difference in OH_{exp} between the model with the plug-flow assumption and two residence time distributions (RTDs, see response to R1.2). These two uncertainty sources are of the order of factors of 1.2 and 1.5, respectively. All of them are comparable or smaller than the difference between measured and modeled OH_{exp} in Li et al. (2015), generally a factor of 2.

Further details are discussed below in response to comments SC.1 and SC.2.

Specific comments

SC.1) The modeling results in Figure 8 of Peng et al. show that up to 90% of the OH in Lambe et al. (2011) is consumed following VOC addition. This result is not consistent with measured OH suppressions conducted by Lambe et al (2012, 2015) that were also discussed in response to an online comment posted by Day et al. (2015) during the open discussion of Lambe et al. (2015). They conducted OH exposure calibrations in the presence of known amounts of added JP-10 and isoprene. Neither of these publications are cited or discussed in Peng et al., nor are they used to evaluate the accuracy of the model that is presented in this manuscript. Lambe et al. (2012) and (2015) specifically state:

- a. Following addition of ~ 55 ppbv JP-10 ($\text{OHR}_{\text{ext}} \sim 31 \text{ s}^{-1}$), OH suppressions were measured that range from ~10% to ~50% at corresponding OH exposures ranging from $2.2 \cdot 10^{12} \text{ molec cm}^{-3} \text{ sec}$ to $1.6 \cdot 10^{11} \text{ molec cm}^{-3} \text{ sec}$ at zero OHR_{ext} respectively.
- b. Following addition of ~462 ppbv isoprene ($\text{OHR}_{\text{ext}} \sim 1136 \text{ s}^{-1}$), no OH suppression was measured relative to the zero OHR_{ext} case over a similar range of OH exposures as in (a).

As stated in response to SC.0, the model for OH_{exp} had already been validated by Li et al. (2015).

In addition, for the JP-10 and isoprene experiments reported in Lambe et al. (2012) and Lambe et al. (2015), respectively, the papers in question did not report sufficient experimental parameters to allow us to perform simulations that could be quantitatively compared with measurements. Following the posting of this short comment, we requested and obtained the necessary parameters for modeling those experiments from Dr. Lambe. We have conducted the relevant simulations and comparisons, and discuss the results in the updated manuscript text quoted below.

We do not believe that it would be reasonable to expect no OH suppression in cases with very high input OHR_{ext} . For this reason we have added additional text and figures to the manuscript

to make clear that OH suppression is *expected* given the nature of the radical chemistry in the OFRs. A complete lack of OH suppression at high OHR_{ext} would be very surprising and inconsistent with the known chemistry.

To address these issues we have expanded and modified the section starting on P3906/L4 to read:

“3.6 Summary of the relationship between OH suppression and OH reactivity

In this section we summarize modeled OH suppressions in a large variety of cases in the space of examined physical conditions, and rationalize these OH suppressions in terms of parameters relevant to OH reactivity. In Sections 3.6.1 and 3.6.2 we relate OH suppression to $\text{OHR}_{\text{int}}/\text{OHR}_{\text{tot}}$ in a more theoretical and fundamental manner. In Section 3.6.3 we use $\text{OHR}_{\text{O}_3}/\text{OHR}_{\text{ext}}$ for a more phenomenological and practical discussion, as both OHR_{O_3} and OHR_{ext} are experimental observables.

3.6.1 Relationship between OH suppression and $\text{OHR}_{\text{int}}/\text{OHR}_{\text{tot}}$

OHR_{tot} in OFRs is of the order of $1\text{--}10^3 \text{ s}^{-1}$, leading to OH lifetimes of $\sim 10^{-3}\text{--}1 \text{ s}$, which is orders of magnitude shorter than the residence time of OFRs, $\sim 10^2 \text{ s}$. Thus we can apply the steady-state approximation to the analysis of OH concentration, i.e.:

$$P = L = \text{OH} \times \text{OHR}_{\text{tot}} = \text{OH} \times (\text{OHR}_{\text{int}} + \text{OHR}_{\text{ext}}), \quad (4)$$

where P and L are the production and loss rates of OH, respectively. This equation can be rearranged as:

$$\text{OH} = P/(\text{OHR}_{\text{int}} + \text{OHR}_{\text{ext}}). \quad (5)$$

In the absence of OHR_{ext} , OH is

$$\text{OH}_0 = P_0/\text{OHR}_{\text{int},0}, \quad (6)$$

where the subscripts denote the case of $\text{OHR}_{\text{ext}} = 0$. Therefore, the measure of OH suppression used in the manuscript, fraction of remaining OH after suppression is

$$\text{rOH}_{\text{exp}} = \frac{\text{OH}}{\text{OH}_0} = \frac{P}{P_0} \times \frac{\text{OHR}_{\text{int},0}}{\text{OHR}_{\text{tot}}} = \frac{P}{P_0} \times \frac{\text{OHR}_{\text{int},0}}{\text{OHR}_{\text{int}}} \times \frac{\text{OHR}_{\text{int}}}{\text{OHR}_{\text{tot}}}. \quad (7)$$

If P and OHR_{int} did not change when OHR_{ext} is added, rOH_{exp} would be

$$\text{rOH}_{\text{exp}} = \frac{\text{OHR}_{\text{int}}}{\text{OHR}_{\text{tot}}}. \quad (8)$$

We refer to this equation as the “simplified model” below. As shown in Fig. 4, $\text{OHR}_{\text{int},0}$ varies on the range $1\text{--}100 \text{ s}^{-1}$ over the very wide range of conditions explored here, with typical values of the order of 20 s^{-1} . Thus based on the simplified model it is expected

that OH suppression will be significant when $\text{OHR}_{\text{ext}} > 20 \text{ s}^{-1}$. We note that the relevant OHR values are the averages over the reactor residence time.

We compare $r\text{OH}_{\text{exp}}$ vs. $\text{OHR}_{\text{int}}/\text{OHR}_{\text{tot}}$ for the simplified and full models in Fig. 11a.

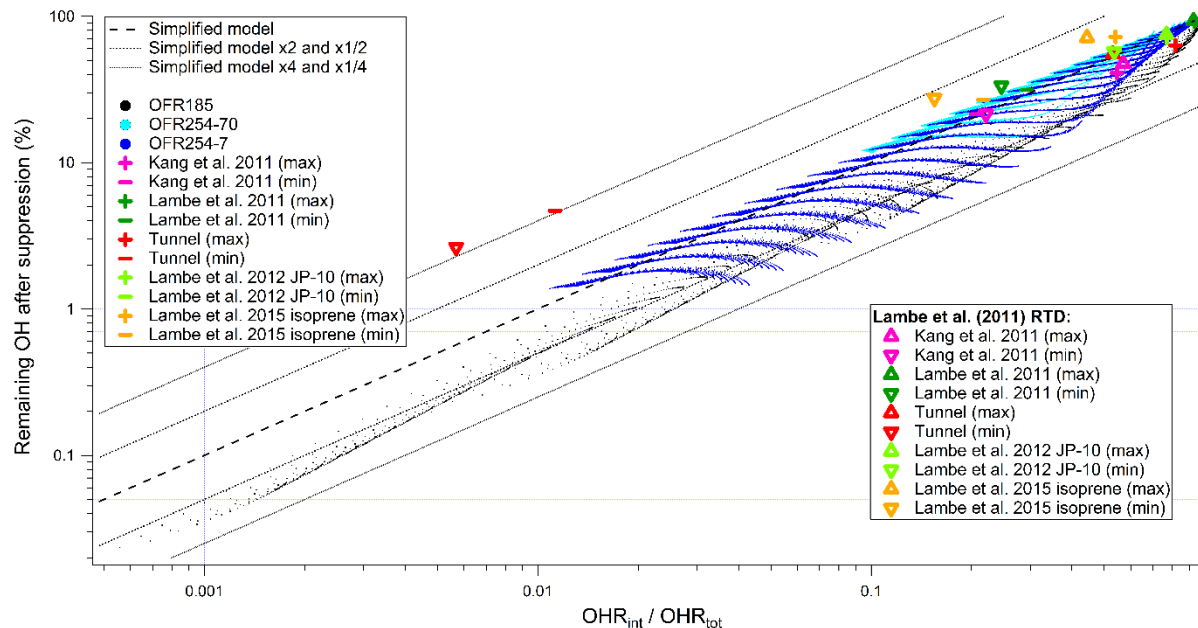


Figure 11a. Percentage of remaining OH after suppression in OFR185 (black dots), OFR254-70 (cyan dots), and OFR254-7 (blue dots) vs. the ratio between internal and total OH reactivities. The “simplified model” (Eq. 8) prediction as well as lines at x2, x4, x1/2, and x1/4 of the simplified model are also shown for comparison. The estimated ranges for laboratory experiments (Kang et al., 2011; Lambe et al., 2011b, 2012, 2015) and a source study in an urban tunnel (Tkacik et al., 2014) are also shown. These ranges are estimated by the models with plug flow and with the Lambe et al. (2011a) residence time distribution according to the experimental conditions in these studies. The lower limit of the percentage of remaining OH after suppression in the tunnel study is notably above the simplified model, since the large amount of NO_x in that case destroys a significant fraction of the internal OH reactants (e.g., O_3 , HO_2 , and OH), leading to $\text{OHR}_{\text{int},0}/\text{OHR}_{\text{int}}$ much higher than 1, while the major contribution of H_2O photolysis to both P and P_0 leads to P/P_0 close to 1.

Results from the full model are close to those of the simplified model, with most datapoints within a factor of 2. This demonstrates that the OH suppression results have a solid theoretical foundation. The ratios of full to simplified model OH suppressions in OFR185, OFR254-70, and OFR254-7 have geometric means of 0.51, 1.02, and 0.90, respectively, and uncertainty factors (see Section 2.3.1) of 1.27, 1.07, and 1.26, respectively. The differences between the full and the simplified models are thus comparable to the uncertainties due to chemical kinetic parameters.

In addition, deviations from the analytical prediction line can also be explained:

- i) OFR185 datapoints are systematically below the simplified model. This results from $\text{OHR}_{\text{int},0}/\text{OHR}_{\text{int}}$ being lower than 1 (Fig. S14), because OHR_{int} increases as the external OH reactant converts OH to HO_2 . P/P_0 is always ~ 1 (Fig. S13) while $\text{OHR}_{\text{int},0}/\text{OHR}_{\text{int}}$ is roughly 0.5 on average, leading to a ratio of ~ 0.5 between the full and simplified model values.
- ii) OFR254 points at low H_2O and/or UV lie across the simplified model prediction. Since, at low H_2O and/or UV, the dominant contribution to both P and OHR_{int} is from O_3 , P and OHR_{int} are both very close to the value at $\text{OHR}_{\text{ext}}=0$ (Figs. S13 and S14), leading to very small deviations from the simplified model prediction. However, the right part of each strip of datapoints in Fig. 11a deviate from the simplified model more significantly. These points correspond to high H_2O and/or UV conditions, where both P and OHR_{int} are higher than P_0 and $\text{OHR}_{\text{int},0}$. P is elevated (by up to $\sim 50\%$) compared to P_0 , as HO_2 , which can be recycled to OH by O_3 , is efficiently produced during the destruction of external OH reactant. OHR_{int} is more elevated (by a factor up to ~ 10) compared to $\text{OHR}_{\text{int},0}$, as not only HO_2 increases, but also H_2O_2 . Thus, the overall product of P/P_0 and $\text{OHR}_{\text{int},0}/\text{OHR}_{\text{int}}$ is < 1 at high H_2O and UV, leading to negative deviations of the corresponding datapoints from the simplified model prediction. Thus in those cases the simplified model *underestimates* OH suppression.

Considering the minor and explainable deviations, we conclude that OH suppression can be estimated within a factor of $\sim 2-3$ as $\text{OHR}_{\text{int}}/\text{OHR}_{\text{tot}}$.

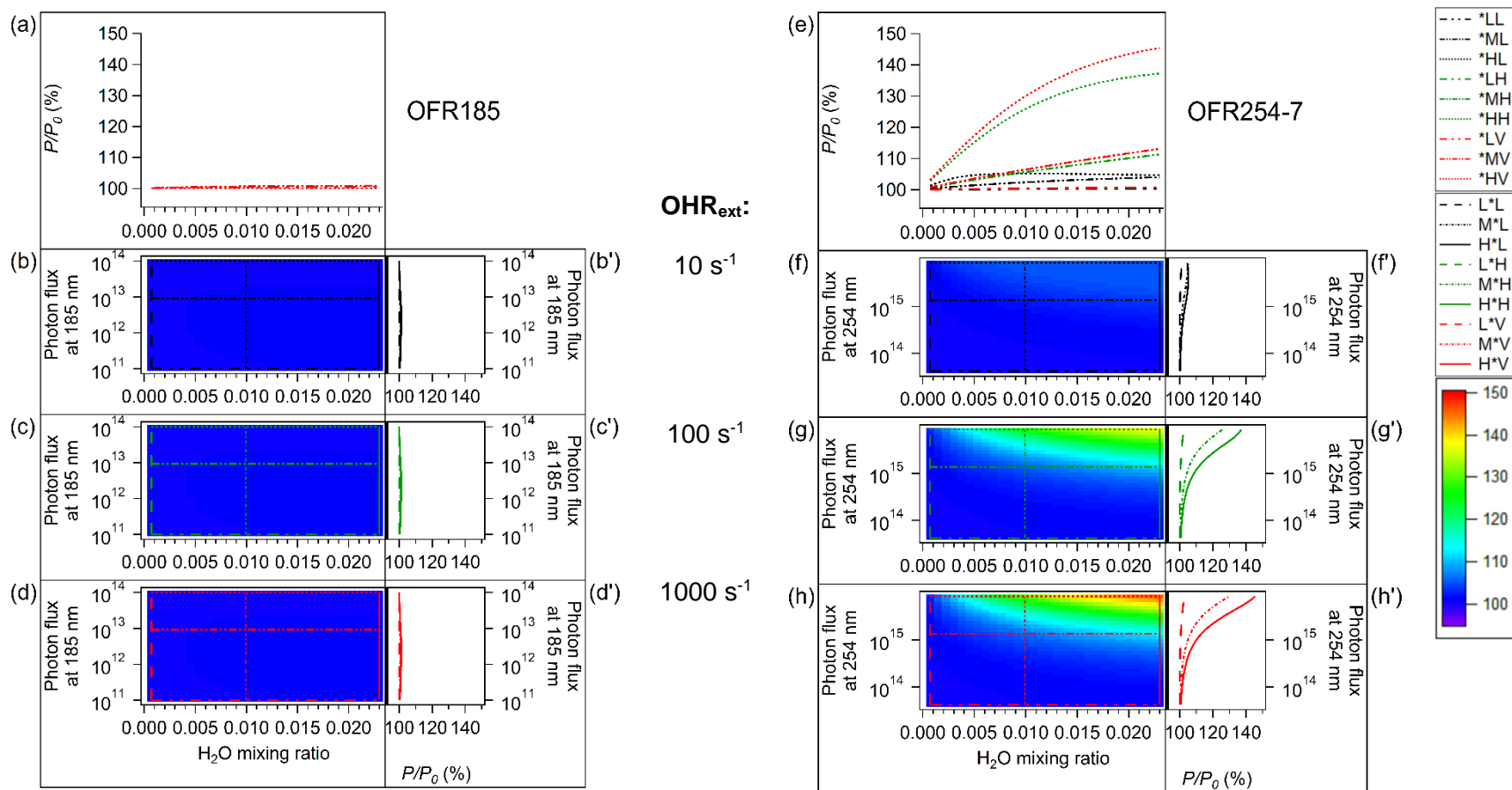


Figure S13. Percentage of OH production rate to that at the same H_2O and UV but $OHR_{ext}=0$ vs. the same parameters and in the same format as Fig. 2.

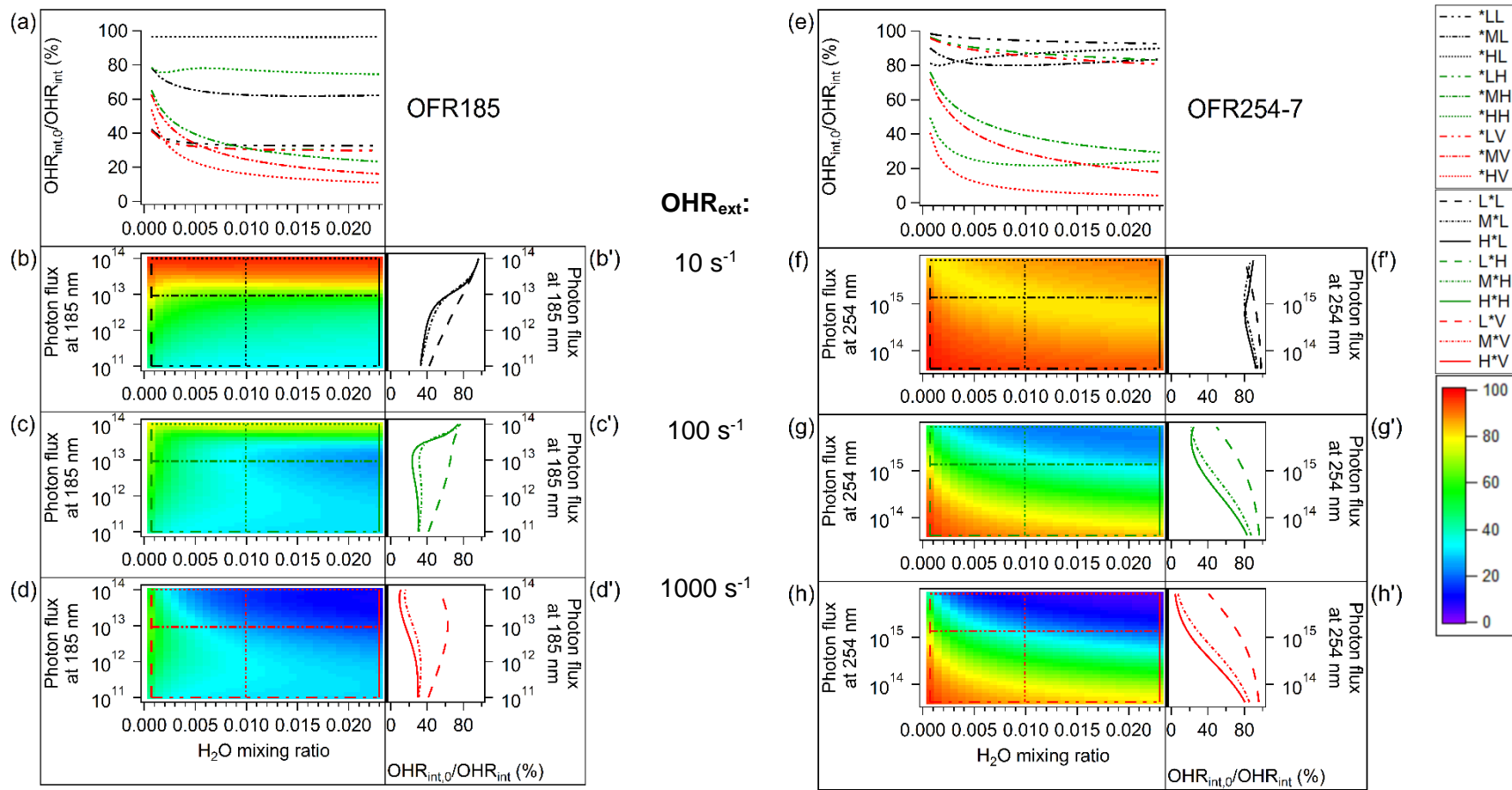


Figure S14. Percentage of OHR_{int} to that at the same H_2O and UV but $OHR_{ext}=0$ vs. the same parameters and in the same format as Fig. 2.

3.6.2 Model-estimated OH suppression for literature studies

To illustrate the range of OH suppressions that may have been present in previous OFR studies, we estimate $r\text{OH}_{\text{exp}}$ and $\text{OHR}_{\text{int}}/\text{OHR}_{\text{tot}}$ in several literature OFR experiments with our model. We strive to include experiments that span a range of different precursors and conditions. We obtained experimental conditions (relative humidity, residence time, OHR_{ext} etc.) from the relevant papers. However, as no information of UV can be found in the selected literature studies, UV is estimated according to literature OH_{exp} . We emphasize that as long as its impact is carefully taken into account, OH suppression is not a “problem” but an “expected feature” of OFR experiments. Only when OH suppression is not taken into account, e.g., when OH_{exp} calibration experiments use OHR_{ext} very different from the experiments of interest, it can result in significant errors in the estimated OH_{exp} . The literature experiments simulated here include two series of OFR254 laboratory experiments with various precursors (Kang et al., 2011; Lambe et al., 2011b), two series of OFR254 laboratory experiments with specific precursors, i.e., JP-10 (tricyclo[5.2.1.0^{2,6}]decane) and isoprene, respectively (Lambe et al., 2012, 2015), and a source study in an urban tunnel using OFR185 (Tkacik et al., 2014). As isoprene reacts very rapidly with OH and may not be well surrogated by SO_2 even when including the OH reactivity of its oxidation products, its chemistry is thus modeled with the semi-explicit scheme in Krechmer et al. (2015). Note that the OH suppressions in the experiments are obtained from the model using the best available information or estimates of the experimental conditions.

The results of the plug-flow model and the model with the RTD reported in Lambe et al. (2011a) are in generally good agreement (Fig. 11a). Both of them suggest that some degree of OH suppression played a role in all investigated previous studies, which is consistent with most of the experimental data available for those experiments. The range of the remaining OH after suppression in the JP-10 experiments of Lambe et al. (2012) is estimated by the model as ~60–70%, in reasonable agreement with the measured values of ~50–90%.

Next we compare the OH remaining reported for the calibration experiments of Tkacik et al. (2014) using NO vs. a modeled range. The comparison is shown Fig. S15. The model reproduces well the OH suppression at lamp voltages of 75 and 110 V, while it overestimates the percentage of remaining OH (i.e., it *underestimates* the OH suppression) at 45 V. The latter lamp voltage is near the threshold of lamp emission and where UV flux is most uncertain and differences between individual lamps can be greatest, so the larger uncertainty in UV may be responsible for the observed differences. If UV at 45 V is reduced by a half, modeled OH suppression is indeed in very good agreement with the measurements.

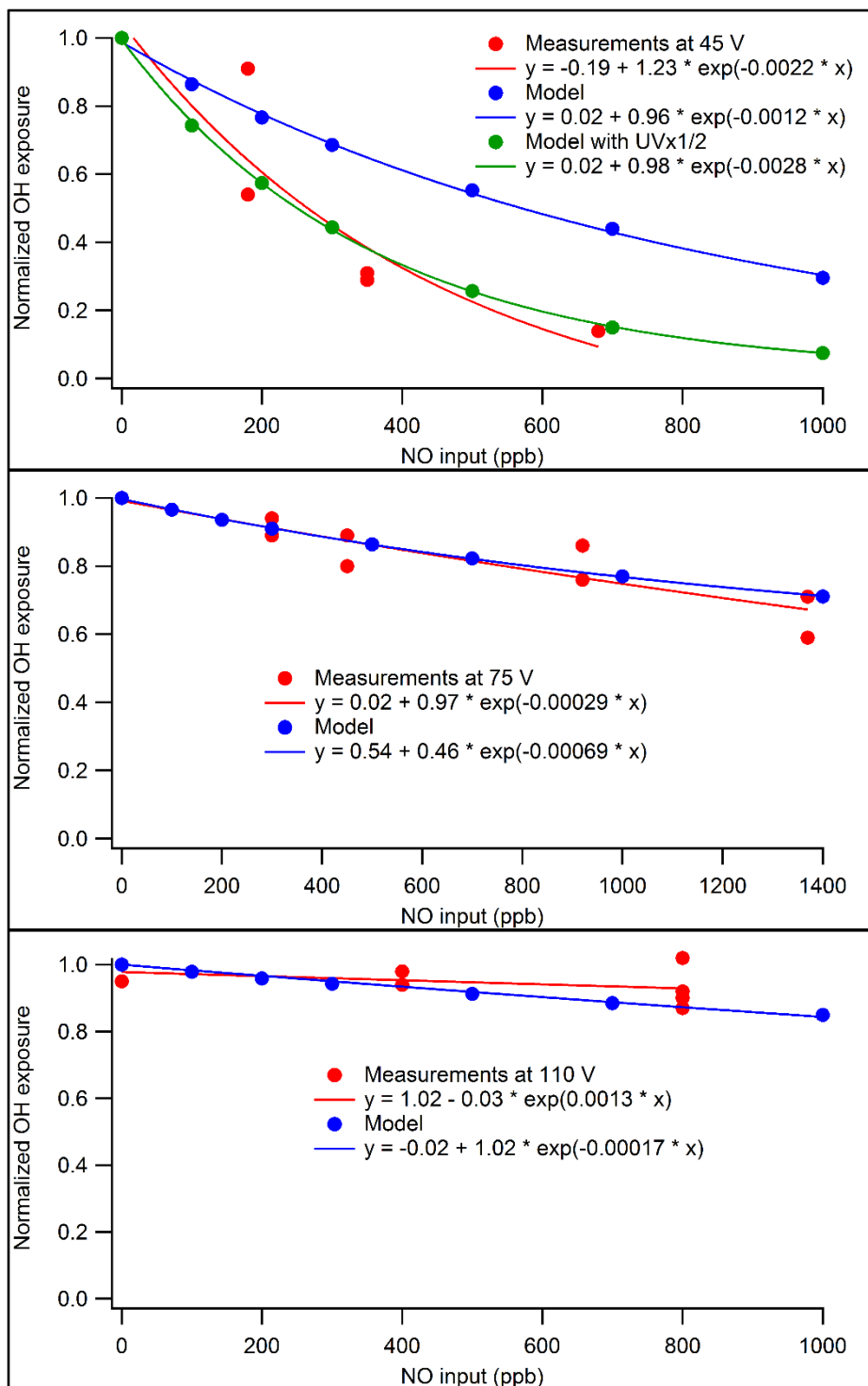


Figure S15. Modeled (blue with full UV and green with half UV) and measured (red; Tkacik et al., 2014) OH exposures in the PAM normalized to that in the case without NO as a function of initial NO input (in ppb) at the lamp voltages of 45 (upper), 75 (middle), and 110 V (lower). Exponential fitting curves for the measurements reported in Tkacik et al. (2014) and the model predictions in this study are also shown.

The modeled OH remaining for the tunnel study (~5–50%, Fig. 11a) is lower than for the calibration cases. Tkacik et al. (2014) only used NO as external OH reactant in their OH_{exp} calibration experiments, while our modeled cases also include CO (measured in Tkacik et al. (2014) but neglected when OHR_{ext} was considered) and VOCs (estimated from their ratios to CO according to Borbon et al. (2013)), which also comprise a large fraction of OHR_{ext}. NO_x is rapidly oxidized to HNO₃ in OFRs (Li et al., 2015) consuming a single OH in the process, and hence is less effective at suppressing OH during most of the residence time. CO and VOCs more effectively reduce OH over the entire residence time, since CO reacts with OH slowly, and many generations of oxidation products of the initial VOCs continue to react with OH. Therefore, although CO and VOCs may appear less important in suppressing OH than NO_x in terms of initial OHR_{ext}, they are actually more important in terms of effective OH reduction or effective OHR_{ext} (averaged over the residence time). If we exclude CO and VOCs from the modeled tunnel cases, the modeled percentage of remaining OH will be ~10–80%, which is consistent with the measured range in the calibration experiments with pure NO in the tunnel study (~20–95%; Lambe, 2015).

Thus the OH_{exp} predicted by the model, which had already been validated by Li et al. (2015), results in OH suppression predictions that are also consistent with most previous literature measurements. There is however one case for which a disagreement between modeled and measured OH suppressions is observed: the isoprene experiments in Lambe et al. (2015). This is observed despite taking into account the expected decrease in OHR_{ext} with OH_{exp} as noted above. Our model suggests a percentage of remaining OH after suppression from ~30% to ~70% in these experiments, while Lambe et al. (2015) reported no measurable OH suppression (based on measurements using SO₂, not isoprene). If OH production is about constant as shown above (Fig. S13), it is virtually impossible to explain (e.g., using Eq. 7) an observation of OH concentration being constant when its lifetime is reduced by a large factor by high OHR_{ext}. One complexity of isoprene chemistry is OH recycling. However, we already include an OH recycling of 6.3% (Liu et al., 2013) for the primary oxidation of isoprene and a full OH recycling for the conversion of isoprene-derived hydroxyhydroperoxides (ISOPOOH) into epoxydiols (IEPOX) (Paulot et al., 2009) in the reaction scheme. The magnitude of the effect of OH recycling of other reactions of isoprene and its oxidation products is much too small to explain the observed deviations. For OH suppression to be negligible, OH recycling would need to be ~100% for isoprene and for many subsequent generations of its oxidation products, which is very unrealistic. Although isoprene chemistry is not known in complete detail, we cannot explain such a large deviation between measurements and model predictions using any known or plausible chemical processes.

In addition, the effect of non-plug flow does not explain the model-measurement discrepancy. As shown in Fig. S16, OH suppression in the literature studies estimated by the model with the Lambe et al. (2011a) RTD is very close to that estimated by the plug-flow model, regardless of what is considered as OH_{exp} in the non-plug-flow model (see Section 3.5) and whether UV is fixed to the value estimated in the plug-flow model.

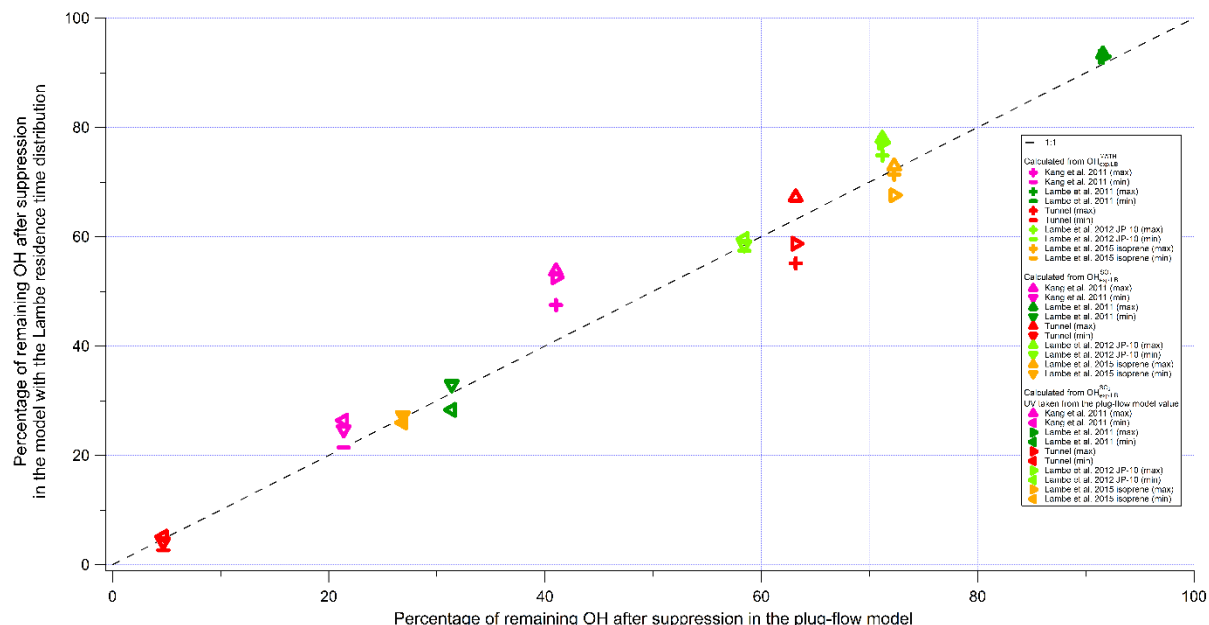


Figure S16. Percentage of remaining OH after suppression in the model with the Lambe et al. (2011a) residence time distribution vs. that in the plug-flow model. The former is calculated from i) directly integrated OH exposure ($\text{OH}_{\text{exp, LB}}^{\text{MATH}}$), ii) OH exposure estimated from SO_2 (as a tracer in most literature experiments) decay ($\text{OH}_{\text{exp, LB}}^{\text{SO}_2}$), and iii) $\text{OH}_{\text{exp, LB}}^{\text{UV}}$ obtained with UV estimated in the plug-flow model.

In summary, the reasons for the model-measurement discrepancy for the case of isoprene remain unclear, and may include contributions from uncertain isoprene chemistry in the model or other model and measurement uncertainties. We suggest that the OH oxidation of isoprene in OFRs be investigated further with a combined model/measurement approach, over a wide range of experimental conditions (initial isoprene, H_2O , and UV) and with direct measurements of isoprene and its oxidation products. If a complete lack of OH suppression is consistently observed in future experiments, its explanation may be of great interest to understand the chemistry of isoprene oxidation.

3.6.3 Relationship between OH suppression and $\text{OHR}_{\text{O}_3}/\text{OHR}_{\text{ext}}$

Although the relationship between $r\text{OH}_{\text{exp}}$ and $\text{OHR}_{\text{int}}/\text{OHR}_{\text{tot}}$ makes clear the origin of OH suppression, neither OHR_{int} nor OHR_{tot} can be easily measured or estimated, because of the short-lived radicals comprising a large fraction of OHR_{int} , i.e., HO_2 and OH, and the difficulty of measuring H_2O_2 . To provide a more practical method to estimate $r\text{OH}_{\text{exp}}$, we show another consistent relationship between $r\text{OH}_{\text{exp}}$ and a quantity related to OHR.”

The rest of the text in this section continues from P3906-L5 in the AMTD manuscript.

The updated version of Figure 8 in the AMTD paper (now Fig. 11b in this document).

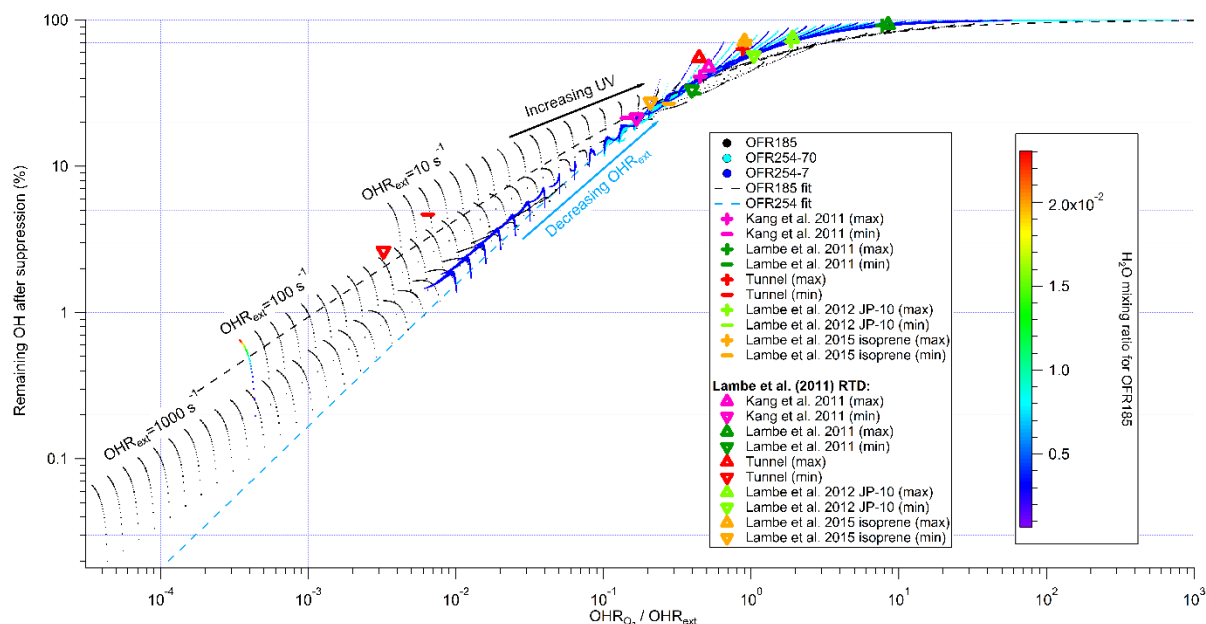


Figure 11b. Percentage of remaining OH after suppression in OFR185 (black dot), OFR254-70 (cyan dots), and OFR254-7 (blue dots) vs. the ratio of OH reactivity from O₃ to external OH reactivity. The fit curves for OFR185 (black dash) and OFR254 (light blue dash) are shown. The estimated ranges for laboratory experiments (Kang et al., 2011; Lambe et al., 2011b, 2012, 2015) and a source study in an urban tunnel (Tkacik et al., 2014) are also shown. These ranges are estimated by the models with plug flow and with the Lambe et al. (2011a) residence time distribution according to the experimental conditions in these studies (see text). The three series of OFR185 data points corresponding to OHR_{ext} = 10, 100, and 1000 s⁻¹ are respectively labeled. A strip of OFR185 data points are colored by H₂O mixing ratio.

We also modify text of P3908/L1 to:

“We also estimate the ranges of rOH_{exp} and OHR_{O_3}/OHR_{ext} of the previous OFR experiments discussed above (Fig. 11b). All estimated values of rOH_{exp} vs. OHR_{O_3}/OHR_{ext} of these experiments follow well this relationship. Most of the estimated values fall into the regime where OH suppression is significant (estimated remaining OH range ~5–70%). This suggests that unless OH_{exp} is calibrated during the relevant experiments by measuring the decay of a reactant, O₃ and OHR_{ext} need to be known to estimate the extent of OH suppression. Using OH_{exp} measured under low OHR_{ext} conditions for experiments at high OHR_{ext} can lead to more than an order-of-magnitude error in the estimated OH_{exp} , even if UV and H₂O are kept constant.”

In addition, we modify the abstract of P3884/L19 to:

“The range of modeled OH suppression for literature experiments is consistent with the measured values except for those with isoprene. The finding on OH suppression may

have important implications for the interpretation of past laboratory studies, as applying OH_{exp} measurements acquired under different conditions could lead to over an order-of-magnitude error in the estimated OH_{exp} .”

SC.2) Another incorrect representation of data is in Figure 8 of Peng et al., which shows that ~92-97% of the OH is suppressed in tunnel measurements conducted by Tkacik et al (2014). OH suppression calibration data is reported in Figures S3 - S6 of the Supporting Information in Tkacik et al. (2014). Following the addition of ~460 ppbv NO, which was the median NO mixing ratio measured by Tkacik et al. (2014), OH suppression ranged from approximately 5% to 80% at corresponding OH exposures ranging from 2.5×10^{12} molec cm^{-3} sec to 5.8×10^{11} molec cm^{-3} sec in the absence of added NO, respectively, and is used to adjusted OH exposure data presented in that paper. As with the data of Lambe et al. (2012, 2015), the OH suppression measurements conducted by Tkacik et al. (2014) are also not discussed or compared with the model results of Peng et al.

First of all, some of the runs for the tunnel data that were included in the AMTD version had a mistake in the input conditions. The updated Fig. 8 of the AMTD paper (Fig. 11 in this document) with the correct inputs is shown above (see response to SC.1). The upper limit of the percentage of remaining OH after suppression for the tunnel study increases from ~9% to ~50%, while the change in its lower limit is minor (from ~3% to ~5%). This range of percentage of remaining OH is still lower than the values reported in Tkacik et al. (2014), ~20–95% (i.e., OH suppression of ~5–80%).

The reason why a difference (but not a discrepancy) remains has been explained in the response to SC.1. In short, the calibration experiments only used NO while the real tunnel air also had important contributions from CO and VOCs to the average OHR_{ext} .

SC.3) The following consideration should have been included in the manuscript of Peng et al.: the plug flow assumption does not represent the PAM conditions (e.g. Fig. 3 in Lambe et al., 2011). In non-pulsed experiments, as are used in OH exposure calibrations, the gas phase concentration includes molecules that have spent a short time in the flow reactor (no recirculation) and molecules that have spent a long time in the flow reactor (recirculated). The majority of the molecules (~85%) spend a shorter time in the reactor than assumed by plug flow and the other ~15% spend a longer time than assumed by plug flow (as estimated from integrating under the CO_2 curve in Fig. 3 of Lambe et al. (2011)). This suggests measured OH suppression values would actually be lower than OH suppression values that are modeled assuming plug flow— a trend that is qualitatively consistent with the measurement/model discrepancies outlined above.

See response to comment R1.2. We also note that the validity of the statement in the comment about “OH suppression values” depends on what is defined as OH_{exp} . If OH_{exp} with the measured RTD is calculated from direct integration, this statement is always true (although the difference is most often small). However, if OH_{exp} is estimated from the decay of species under

study, as recommended in the response to comment R1.2, this statement is not necessarily true, since less SO₂ consumption leads to a lower OH_{exp,RTD}^{SO₂}.

References

Borbon, A., Gilman, J. B., Kuster, W. C., Grand, N., Chevaillier, S., Colomb, A., Dolgorouky, C., Gros, V., Lopez, M., Sarda-Estevé, R., Holloway, J., Stutz, J., Petetin, H., McKeen, S., Beekmann, M., Warneke, C., Parrish, D. D. and De Gouw, J. A.: Emission ratios of anthropogenic volatile organic compounds in northern mid-latitude megacities: Observations versus emission inventories in Los Angeles and Paris, *J. Geophys. Res. Atmos.*, 118(4), 2041–2057, doi:10.1002/jgrd.50059, 2013.

George, I. J., Vlasenko, A., Slowik, J. G., Broekhuizen, K. and Abbatt, J. P. D.: Heterogeneous oxidation of saturated organic aerosols by hydroxyl radicals: uptake kinetics, condensed-phase products, and particle size change, *Atmos. Chem. Phys.*, 7(16), 4187–4201, doi:10.5194/acp-7-4187-2007, 2007.

Kang, E., Toohey, D. W. and Brune, W. H.: Dependence of SOA oxidation on organic aerosol mass concentration and OH exposure: experimental PAM chamber studies, *Atmos. Chem. Phys.*, 11(4), 1837–1852, doi:10.5194/acp-11-1837-2011, 2011.

Krechmer, J. E., Coggon, M. M., Massoli, P., Nguyen, T. B., Crounse, J. D., Hu, W., Day, D. A., Tyndall, G. S., Henze, D. K., Rivera-Rios, J. C., Nowak, J. B., Kimmel, J. R., Mauldin, R. L., Stark, H., Jayne, J. T., Sipilä, M., Junninen, H., Clair, J. M. St., Zhang, X., Feiner, P. A., Zhang, L., Miller, D. O., Brune, W. H., Keutsch, F. N., Wennberg, P. O., Seinfeld, J. H., Worsnop, D. R., Jimenez, J. L. and Canagaratna, M. R.: Formation of Low Volatility Organic Compounds and Secondary Organic Aerosol from Isoprene Hydroxyhydroperoxide Low-NO Oxidation, *Environ. Sci. Technol.*, 49(17), 10330–10339, doi:10.1021/acs.est.5b02031, 2015.

Lambe, A. T.: Interactive comment on “Comparison of secondary organic aerosol formed with an aerosol flow reactor and environmental reaction chambers: effect of oxidant concentration, exposure time and seed particles on chemical composition and yield” by A. T. Lambe et, *Atmos. Chem. Phys. Discuss.*, 14, C12169 [online] Available from: www.atmos-chem-phys-discuss.net/14/C12169/2015/, 2015.

Lambe, A. T., Ahern, A. T., Williams, L. R., Slowik, J. G., Wong, J. P. S., Abbatt, J. P. D., Brune, W. H., Ng, N. L., Wright, J. P., Croasdale, D. R., Worsnop, D. R., Davidovits, P. and Onasch, T. B.: Characterization of aerosol photooxidation flow reactors: heterogeneous oxidation, secondary organic aerosol formation and cloud condensation nuclei activity measurements, *Atmos. Meas. Tech.*, 4(3), 445–461, doi:10.5194/amt-4-445-2011, 2011a.

Lambe, A. T., Chhabra, P. S., Onasch, T. B., Brune, W. H., Hunter, J. F., Kroll, J. H., Cummings, M. J., Brogan, J. F., Parmar, Y., Worsnop, D. R., Kolb, C. E. and Davidovits, P.: Effect of oxidant concentration, exposure time, and seed particles on secondary organic aerosol chemical composition and yield, *Atmos. Chem. Phys.*, 15(6), 3063–3075, doi:10.5194/acp-15-

3063-2015, 2015.

Lambe, A. T., Onasch, T. B., Croasdale, D. R., Wright, J. P., Martin, A. T., Franklin, J. P., Massoli, P., Kroll, J. H., Canagaratna, M. R., Brune, W. H., Worsnop, D. R. and Davidovits, P.: Transitions from functionalization to fragmentation reactions of laboratory secondary organic aerosol (SOA) generated from the OH oxidation of alkane precursors., *Environ. Sci. Technol.*, 46(10), 5430–7, doi:10.1021/es300274t, 2012.

Lambe, A. T., Onasch, T. B., Massoli, P., Croasdale, D. R., Wright, J. P., Ahern, A. T., Williams, L. R., Worsnop, D. R., Brune, W. H. and Davidovits, P.: Laboratory studies of the chemical composition and cloud condensation nuclei (CCN) activity of secondary organic aerosol (SOA) and oxidized primary organic aerosol (OPOA), *Atmos. Chem. Phys.*, 11(17), 8913–8928, doi:10.5194/acp-11-8913-2011, 2011b.

Li, R., Palm, B. B., Ortega, A. M., Hu, W., Peng, Z., Day, D. A., Knote, C., Brune, W. H., de Gouw, J. and Jimenez, J. L.: Modeling the radical chemistry in an Oxidation Flow Reactor (OFR): radical formation and recycling, sensitivities, and OH exposure estimation equation, *J. Phys. Chem. A*, 119(19), 4418–4432, doi:10.1021/jp509534k, 2015.

Liu, Y. J., Herdlinger-Blatt, I., McKinney, K. a. and Martin, S. T.: Production of methyl vinyl ketone and methacrolein via the hydroperoxyl pathway of isoprene oxidation, *Atmos. Chem. Phys.*, 13(11), 5715–5730, doi:10.5194/acp-13-5715-2013, 2013.

Mory, M.: *Fluid Mechanics for Chemical Engineering*, John Wiley & Sons, Inc., Hoboken, NJ USA., 2013.

Ortega, A. M., Day, D. A., Cubison, M. J., Brune, W. H., Bon, D., de Gouw, J. A. and Jimenez, J. L.: Secondary organic aerosol formation and primary organic aerosol oxidation from biomass-burning smoke in a flow reactor during FLAME-3, *Atmos. Chem. Phys.*, 13(22), 11551–11571, doi:10.5194/acp-13-11551-2013, 2013.

Ortega, A. M., Hayes, P. L., Peng, Z., Palm, B. B., Hu, W., Day, D. A., Li, R., Cubison, M. J., Brune, W. H., Graus, M., Warneke, C., Gilman, J. B., Kuster, W. C., de Gouw, J. A. and Jimenez, J. L.: Real-time measurements of secondary organic aerosol formation and aging from ambient air in an oxidation flow reactor in the Los Angeles area, *Atmos. Chem. Phys. Discuss.*, 15(15), 21907–21958, doi:10.5194/acpd-15-21907-2015, 2015.

Palm, B. B., Campuzano-Jost, P., Ortega, A. M., Day, D. A., Karl, T., Kaser, L., Jud, W., Hansel, A., Fry, J. L., Brown, S. S., Zarzana, K. J., Dube, W. P., Wagner, N. L., Draper, D. C., Hunter, J. F., Kroll, J. H., Brune, W. H. and Jimenez, J. L.: Real-time organic aerosol formation and oxidative aging using a flow reactor in a pine forest, *Atmos. Chem. Phys. Discuss.*, In press, 2015.

Paulot, F., Crouse, J. D., Kjaergaard, H. G., Kurten, A., St. Clair, J. M., Seinfeld, J. H. and Wennberg, P. O.: Unexpected Epoxide Formation in the Gas-Phase Photooxidation of Isoprene, *Science (80-)*, 325(5941), 730–733, doi:10.1126/science.1172910, 2009.

Peng, Z., Day, D. A., Ortega, A. M., Palm, B. B., Hu, W. W., Stark, H., Li, R., Tsigaridis, K.,

Brune, W. H. and Jimenez, J. L.: Non-OH chemistry in oxidation flow reactors for the study of atmospheric chemistry systematically examined by modeling, *Atmos. Chem. Phys. Discuss.*, 15(17), 23543–23586, doi:10.5194/acpd-15-23543-2015, 2015.

Tkacik, D. S., Lambe, A. T., Jathar, S., Li, X., Presto, A. A., Zhao, Y., Blake, D., Meinardi, S., Jayne, J. T., Croteau, P. L. and Robinson, A. L.: Secondary Organic Aerosol Formation from in-Use Motor Vehicle Emissions Using a Potential Aerosol Mass Reactor., *Environ. Sci. Technol.*, 48(19), 11235–42, doi:10.1021/es502239v, 2014.